

Article

Experimental Study on the Damage and Failure Characteristics of High-Temperature Granite after Liquid-Nitrogen Cooling

Chengzheng Cai ^{1,2,3,*} , Bo Wang ², Zengxin Zou ^{2,3}, Yinrong Feng ² and Zhixiang Tao ²

¹ State Key Laboratory of Intelligent Construction and Healthy Operation & Maintenance of Deep Underground Engineering, China University of Mining and Technology, Xuzhou 221116, China

² School of Mechanics and Civil Engineering, China University of Mining and Technology, Xuzhou 221116, China; ts22030016a31@cumt.edu.cn (B.W.); ts21030036a31@cumt.edu.cn (Z.Z.); ts20030003a31@cumt.edu.cn (Y.F.); ts20030018a31@cumt.edu.cn (Z.T.)

³ School of Low-Carbon Energy and Power Engineering, China University of Mining and Technology, Xuzhou 221116, China

* Correspondence: caicz@cumt.edu.cn

Abstract: To analyze the influence of liquid-nitrogen cooling on the damage and failure of high-temperature granite, granite samples were heated to 150~600 °C for natural cooling and liquid-nitrogen cooling treatment. Brazilian splitting tests were carried out as the samples returned to room temperature, and basic tensile and energy evolution parameters were obtained. Acoustic emission signal parameters during loading were recorded. The experimental results showed that the heating process caused damage to the granite samples, and liquid-nitrogen cooling further increased the degree of damage. Specifically, the ultrasonic velocity of liquid-nitrogen-cooled samples was lower than that of naturally cooled samples at each heating temperature. With an increase in heating temperature, the AE ring-down counts of liquid-nitrogen-cooled samples were higher than that of naturally cooled samples. At the same heating temperature, the dissipated energy of naturally cooled samples was greater than that of liquid-nitrogen-cooled samples. Liquid-nitrogen cooling could effectively promote the propagation of microcracks inside high-temperature granite and result in a reduction in the mechanical strength of granite, which could be conducive to the efficient fracture of high-temperature rock during fracturing.

Keywords: high-temperature granite; hot dry rock; liquid-nitrogen cooling; damage



Citation: Cai, C.; Wang, B.; Zou, Z.; Feng, Y.; Tao, Z. Experimental Study on the Damage and Failure Characteristics of High-Temperature Granite after Liquid-Nitrogen Cooling. *Processes* **2023**, *11*, 1818. <https://doi.org/10.3390/pr11061818>

Academic Editors: Lei Qin and Ruiyue Yang

Received: 11 May 2023

Revised: 11 June 2023

Accepted: 13 June 2023

Published: 15 June 2023



Copyright: © 2023 by the authors. Licensee MDPI, Basel, Switzerland. This article is an open access article distributed under the terms and conditions of the Creative Commons Attribution (CC BY) license (<https://creativecommons.org/licenses/by/4.0/>).

1. Introduction

Geothermal energy exists in the form of heat energy in the lava inside the Earth. Due to its green, low-carbon, renewable, and recycled characteristics, it is a potentially clean source of energy [1]. Due to the high density and low permeability of the dry hot rock (HDR) reservoir, it is necessary to increase the permeability of the reservoir by manual stimulation and improve the surface area of cracks as much as possible to facilitate heat recovery. Therefore, the development of HDR resources consists of two important stages: reservoir fracturing and geothermal exploitation [2]. The process of reservoir fracturing creates a pathway to extract heat energy from a high-temperature rock mass with low permeability. At present, the main way to fracture geothermal HDR resources is hydraulic fracturing. Hydraulic fracturing uses fracturing fluid to crack reservoir rock by injecting high-pressure fracturing fluid through the wellbore into deep reservoir rocks, producing artificial fractures. However, there are some problems with traditional hydraulic fracturing, such as high fracture-pressure formation, pore blockage caused by formation water sensitivity, and large water consumption [3–5]. To solve these problems, researchers have proposed the technical idea of waterless fracturing. Compared with conventional hydraulic fracturing, waterless fracturing is not restricted by water resources, which not only increases the flowback

rate of fracturing fluid and reduces the damage to high-temperature reservoirs caused by fracturing fluid, but also reduces the water resource waste.

Liquid nitrogen, as a cryogenic liquid, can reach $-196\text{ }^{\circ}\text{C}$ under atmospheric pressure, which has obvious advantages in deep thermal reservoirs. When liquid nitrogen is injected into a reservoir, the tensile stress generated by contact with high-temperature rocks will cause thermal cracks [6], forming a complex fracture network. Therefore, the research on HDR reservoir fracturing using liquid nitrogen is expected to provide the theoretical basis for the exploitation and utilization of HDR resources. As a fracturing fluid, liquid nitrogen has been widely used in oil and gas engineering [7]. In the late 20th century, liquid nitrogen was successfully applied to the Devonian shale reservoir with low permeability, which greatly improved reservoir permeability and gas production. This method was further applied to unconventional fracturing in the United States [8,9].

For liquid-nitrogen fracturing technology, the key is that the ultra-low-temperature property of liquid nitrogen can effectively reduce the mechanical properties of rock, therefore improving the subsequent fracturing performance. McDaniel et al. [8] pointed out that when liquid nitrogen is injected into high-temperature reservoirs, a strong thermal shock is generated on the rock surface of the reservoir, inducing the generation and expansion of fractures. Additionally, the freezing effect of fluids in the reservoir after contact with liquid nitrogen also improved the permeability of the reservoir. Ren et al. [10] carried out an experimental study on cryogenic shock on coal caused by liquid nitrogen, and the results showed that the permeability of coal increased after cryogenic shock. To study the influence of liquid-nitrogen cooling on the physical properties of coal, sandstone, and shale, Cai et al. [11–14] compared the change law of the physical and mechanical parameters of the same sample before and after liquid-nitrogen cooling with nuclear magnetic resonance (NMR) and other technologies, and found that liquid-nitrogen cooling could cause freezing damage to rock samples and produce thermal cracks. Liquid-nitrogen cooling induced crack propagation inside the rock sample and the permeability of the treated rock sample was enhanced. Cha et al. [15] conducted a feasibility investigation of cryogenic fracturing for reservoir stimulation using a self-designed experimental device. The results showed that the temperature gradient generated by liquid nitrogen could change the pore structure inside the rock, resulting in many microcracks. Furthermore, the performance of liquid-nitrogen fracturing under true triaxial confining pressure was studied, and it was found that after liquid-nitrogen fracturing, the direction of the principal fracture did not necessarily follow the direction of the principal stress [16,17]. Zhai et al. [18,19] proposed a method for cracking coal using liquid-nitrogen cyclic injection and found that the increase in the effective porosity and the total porosity of coal were positively correlated with freezing time and freezing cycles. Yao et al. [20] demonstrated that the injection of low-temperature and high-pressure fluid was beneficial to reservoir permeability. By numerical simulation, Zhang et al. [21,22] calculated the distribution law of heat conduction and thermal stress in HDR during the liquid-nitrogen jetting process. The results showed that the huge thermal stress generated by a temperature gradient could reduce rock fracture pressure and generate thermal cracks. Yang et al. [23] conducted gas fracturing tests on granite treated with liquid nitrogen and proved that liquid-nitrogen treatment had a significant influence on the fracture pressure of rock samples. Wu et al. [24–26] tested the physical and mechanical properties of granite at different heating temperatures after different cooling methods. They found that cyclic liquid-nitrogen cooling treatment would aggravate the degree of damage to granite. Hong et al. [27] indicated that cyclic liquid-nitrogen fracturing could further reduce the breakdown pressure of high-temperature granite and create complex fractures.

To explore the fracturing effect of different fluids on high-temperature rock, it is necessary to obtain the mechanical properties and failure characteristics of high-temperature rock under external loads. Because high-temperature rocks with different temperatures cannot be directly obtained under laboratory conditions, they are generally prepared by heating normal-temperature rocks. In the heating process, the mineral components inside the rock expand. In addition, when the hot rock is cooled, the mineral components of the

hot rock undergo a process of shrinkage deformation, which will also affect the mechanical properties of the rock. Therefore, to better analyze the influence of liquid-nitrogen cooling on the deformation and failure of high-temperature granite, the granite was heated to 150–600 °C and treated with different cooling methods (liquid-nitrogen cooling and natural cooling); then, relevant tests were carried out. The influence of liquid-nitrogen cooling on mechanical parameters, deformation parameters, acoustic emission (AE) parameters, and energy parameters of high-temperature granite was analyzed, and the corresponding mechanical mechanism was discussed. This research was expected to provide the theoretical basis for the investigation of the mechanism of high-temperature granite failure induced by high-pressure liquid nitrogen.

2. Materials and Methods

2.1. Sample Preparation

To study the influence of liquid nitrogen on the damage and failure characteristics of HDR rocks, outcrop granite samples were collected from Shandong Province, China. Granite is a typical igneous rock, with uniform mineral particles and coarse–medium granular structure. It has a dense structure and hard texture. According to the requirements of the Brazilian splitting test, the granite samples were uniformly processed into cylinders of 50 mm diameter and 25 mm height, as shown in Figure 1. Then, the end surfaces were polished with a fine grinding wheel to ensure that flatness and parallelism was within ± 0.03 mm and ± 0.05 mm, respectively. To reduce the influence of granite heterogeneity on the experimental results, all samples were tested for density and ultrasonic velocity in advance. The samples with close density and ultrasonic velocity were selected as the test objects.



Figure 1. Test rock sample.

2.2. Test Equipment

In the process of this test, the physical and mechanical properties of granite at different temperatures before and after natural cooling and liquid-nitrogen cooling were measured. The physical parameter was mainly longitudinal wave velocity, and the measured mechanical parameters included tensile strength, deformation parameters, AE parameters, etc. As shown in Figure 2, the test equipment used included an NM-4A non-metallic ultrasonic detection analyzer, a low-temperature liquid-nitrogen tank, an MXQ1700 Muffle furnace, a CSS-88020 electronic universal test machine, a PCI-2 AE system, etc.

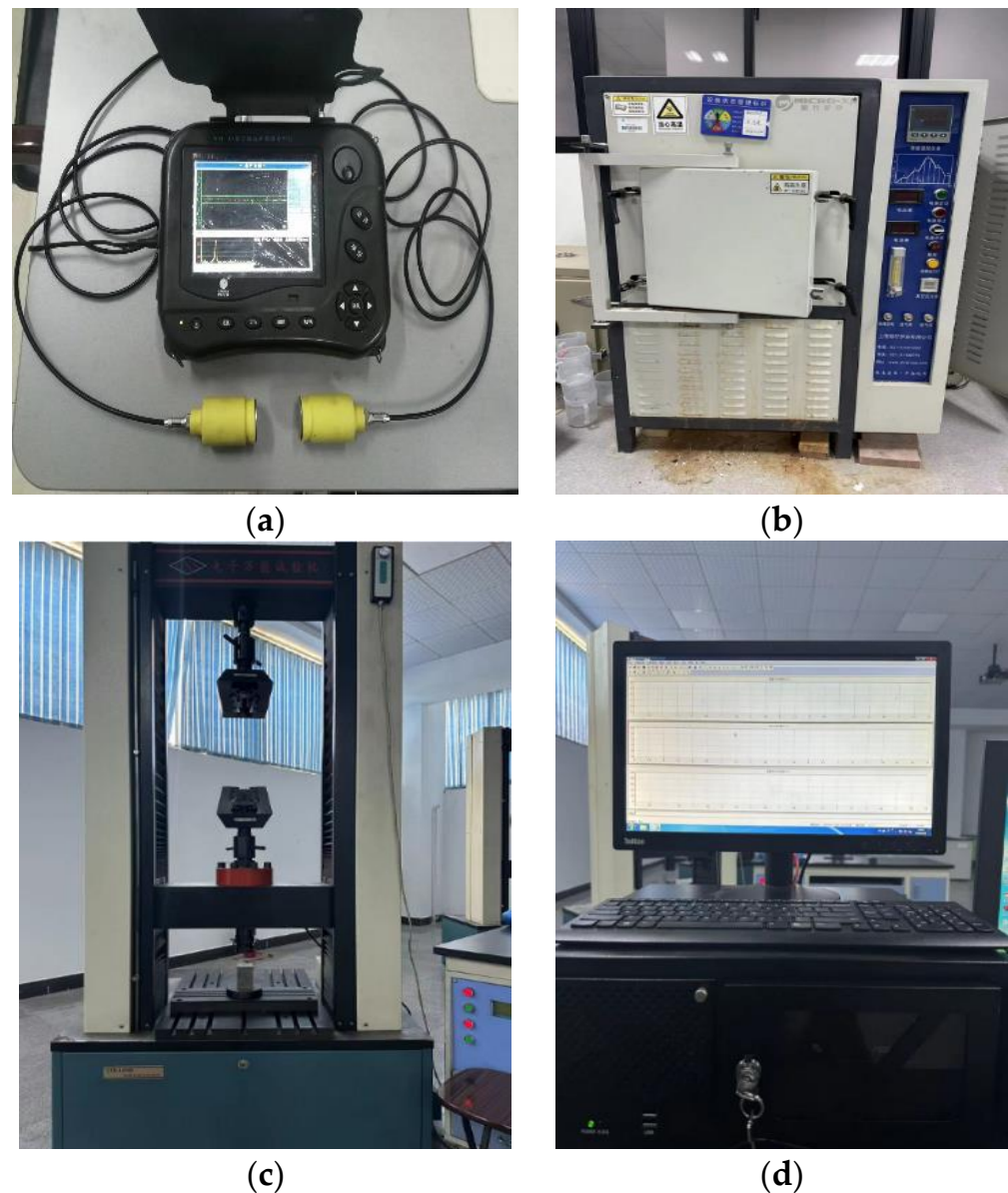


Figure 2. Photograph of the test equipment: (a) ultrasonic detection analyzer; (b) MXQ1700 Muffle furnace; (c) CSS-88020 electronic universal test machine; (d) PCI-2 AE system.

As shown in Figure 3, the experimental operation and equipment performance were as follows:

1. Ultrasonic test. The NM-4A non-metallic ultrasonic detector was used to acquire the ultrasonic velocity of the high-temperature granite before and after natural cooling and liquid-nitrogen cooling treatment. Each sample was measured three times, and the average value was taken as the ultrasonic velocity. According to the variation of ultrasonic velocity, the degree of damage to the granite can be preliminarily estimated.
2. Heating treatment. Because granite samples were prepared in a room-temperature environment, high-temperature rock samples with different initial temperatures cannot be directly obtained. Therefore, to carry out the related tests of high-temperature granite, samples should be heated to a predetermined temperature first, and then the effect of liquid-nitrogen cooling on the physical and mechanical properties can be evaluated. The heating equipment used in the test process was the MXQ1700 Muffle furnace. The maximum heating temperature of the furnace was 1600 °C, which

- allowed adjustment to the heating rate according to the test requirements. The heating rate used in this test was $4\text{ }^{\circ}\text{C}/\text{min}$.
3. **Cooling treatment.** The high-temperature granite was cooled in two ways: natural cooling and liquid-nitrogen cooling. For natural cooling, the high-temperature granite was restored to normal temperature in air. For liquid-nitrogen cooling, the high-temperature granite was submerged in a liquid-nitrogen tank for full cooling. Because the natural cooling and liquid-nitrogen cooling treatments of granite samples experienced the same heating process, the effect of liquid-nitrogen cooling on the mechanical properties and failure characteristics of high-temperature granite could be effectively evaluated by comparing the change trends of the related parameters samples with the same heating temperature.
 4. **Brazilian splitting tests.** The granite samples cooled naturally and with liquid nitrogen were loaded into the CSS-88020 electronic universal test machine to obtain the load–displacement curves and tensile strength. The experimental machine can conduct mechanical tests of nonlinear materials, such as rock and concrete. The maximum applied load was 100 KN and the displacement accuracy was 0.001 mm. The loading rate was adjusted by the device’s system. The displacement loading mode used in this work and the loading rate was 0.05 mm/min. During the loading process, the load, displacement, and other parameters of samples were recorded in real time.
 5. **AE test.** In the process of rock deformation and failure, the release of strain energy will produce AE signals. The real-time rupture characteristics of the rock can be obtained by the acquisition, analysis, and processing of AE signals, which can provide a basis for the subsequent analysis of mechanical properties. During the Brazilian splitting tests, the PCI-2 AE monitoring system was used to synchronously record the AE signals of the granite. The equipment is mainly composed of an AE probe, 8-channel PC-8 AE plate, preamplifier, waveform and filter module, energy module, and acoustic transmission signal receiver and analysis module. The signal acquisition frequency was 0.001–3 MHz and the maximum threshold value of the signal was 100 dB, to reduce the influence of environmental noise on the test results and ensure enough AE signals were being collected. The AE threshold value set in this test was 40 dB, and the signal acquisition frequency was 0.14 MHz.

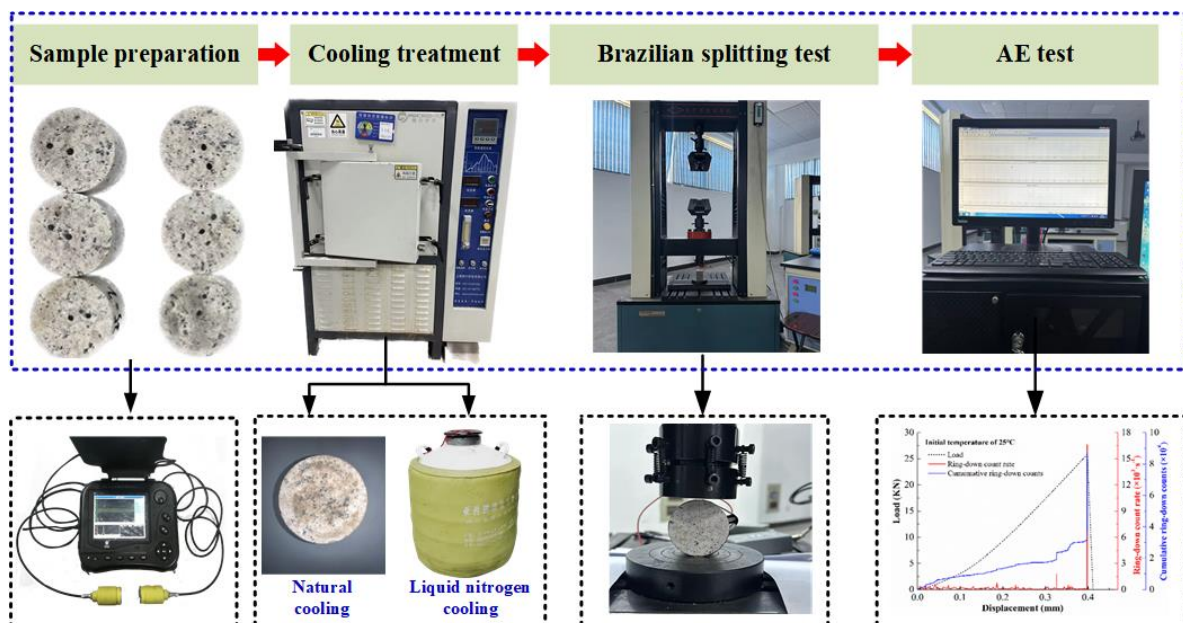


Figure 3. Experimental items.

2.3. Test Method

Because high-temperature granite cannot be obtained directly, the initial samples were heated to prepare high-temperature granite samples with different initial temperatures. When the samples were heated to the predetermined temperature, they were subjected to natural cooling and liquid-nitrogen cooling treatments. All the heating and cooling treatment processes are shown in Figure 4. In summary, the rock samples used in the test comprise the following two types: naturally cooled samples and liquid-nitrogen-cooled samples. The naturally cooled samples were heated to the predetermined temperature, and then naturally cooled to room temperature before the ultrasonic, Brazilian splitting, and AE tests. The samples went through two stages: heating and natural cooling. With respect to the liquid-nitrogen-cooled samples, the samples were heated to the predetermined temperature and then put into the liquid-nitrogen tank for 2 h. After the samples were removed from the liquid nitrogen and returned to room temperature, the relevant tests were conducted. In this process, they went through two stages: heating and liquid-nitrogen cooling. However, before the follow-up tests, the samples taken from liquid nitrogen increased to room temperature in air conditions, and the samples went through a heating stage from liquid-nitrogen temperature to room temperature. Therefore, compared with the naturally cooled samples, the liquid-nitrogen-cooled samples went through two heating stages.

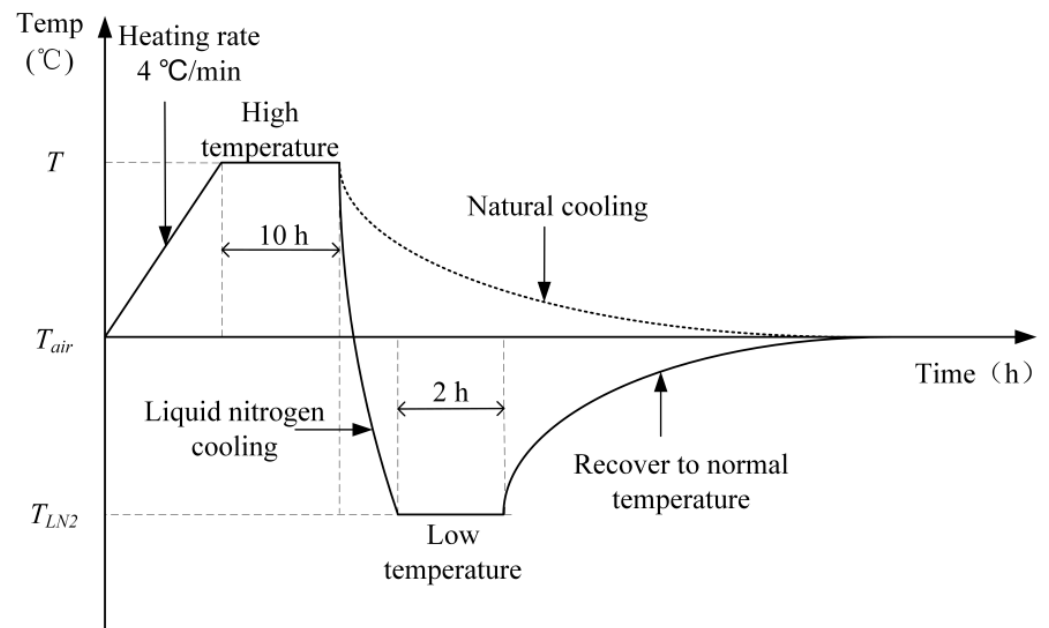


Figure 4. Schematic diagram of heating and cooling treatment process.

The heating process of granite was accompanied by water evaporation and mineral deformation, which affected its mechanical properties. Therefore, to better evaluate the influence of liquid-nitrogen cooling on the mechanical properties of high-temperature granite, tests were, respectively, performed on naturally cooled and liquid-nitrogen-cooled samples. Based on the measured parameters of these two types of samples, the influence of liquid-nitrogen cooling on the damage and failure characteristics of high-temperature granite was comprehensively evaluated.

In this work, five heating temperatures (including room temperature) and two cooling treatments were designed. In total, 10 groups of tests were carried out. During the heating process, the heating rate was kept below 5 °C/min to reduce the influence of the heating process on the initial damage state of rock samples.

The prepared granite samples were numbered and grouped as shown in Table 1. The naturally cooled and liquid-nitrogen-cooled samples were labeled as “heating temperature-

A-number" and "heating temperature-L-number[#]", respectively. The letters on the label represented the cooling treatment (A—natural cooling; L—liquid-nitrogen cooling). The "[#]" was just a symbol, it had no specific meaning. Before the formal experiments, the size and weight of each granite sample was measured, and the initial ultrasonic velocities of all samples were tested. Each sample was tested three times, and the average value was taken as the initial ultrasonic velocity value. Ultrasonic and Brazilian splitting tests were conducted on different cooling treatment samples. After the samples were slowly heated to 150–600 °C, natural cooling and liquid-nitrogen cooling treatments were conducted, respectively. Then, ultrasonic and Brazilian splitting tests were performed. The heating rate during heating was less than 5 °C/min. The total heating and holding time was 10 h.

Table 1. Group grouping and treatment methods of rock samples.

Rock Sample Type	Heating Temperature (°C)	Number	Process Mode
Naturally cooled sample	25	25-A-1 [#] , 25-A-2 [#]	After heating to the target temperature, cooled naturally to room temperature
	150	150-A-1 [#] , 150-A-2 [#]	
	300	300-A-1 [#] , 300-A-2 [#]	
	450	450-A-1 [#] , 450-A-2 [#]	
	600	600-A-1 [#] , 600-A-2 [#]	
Liquid-nitrogen-cooled sample	25	25-L-1 [#] , 25-L-2 [#]	Return to normal temperature after cooling with liquid nitrogen
	150	150-L-1 [#] , 150-L-2 [#]	
	300	300-L-1 [#] , 300-L-2 [#]	
	450	450-L-1 [#] , 450-L-2 [#]	
	600	600-L-1 [#] , 600-L-2 [#]	

3. Results

3.1. Change in Ultrasonic Velocity

Ultrasonic technology is an important means to detect rock damage, and the propagation speed of ultrasonic waves in solids, liquids, and gases is successive. Ultrasonic waves propagate very fast in a rock matrix. When cracks are located in the propagation routine of ultrasonic waves, ultrasonic velocity will decrease. Therefore, the ultrasonic velocity of rock is closely related to the closing, opening, and expansion of primary fissures. In general, when ultrasonic velocity drops, new fissures are created inside the rock. Ultrasonic waves can be divided into transverse waves, longitudinal waves, torsion waves, ram waves, and surface waves according to their propagation direction and the vibration of the particles of the propagation medium. In these types of waves, the propagation mechanism of the longitudinal wave is controlled by the volume of the medium, and it shows different propagation velocities in solids, liquids, and gases. Based on this point, longitudinal waves were chosen for the analysis of the influence of liquid nitrogen on high-temperature granite.

During the preparation of the high-temperature granite, a certain degree of damage will be introduced into the sample during heating, which will lead to a change in physical and mechanical properties. Therefore, to better analyze the cracking effects of the cooling methods on high-temperature granite, the relevant parameters of liquid-nitrogen-cooled and naturally cooled samples were compared, to evaluate the cryogenic cracking effect of liquid-nitrogen. Ultrasonic waves are important for testing rock damage indirectly. The propagation velocity of ultrasonic waves in a solid is higher than in air. Therefore, when new cracking occurs in rock, ultrasonic velocity will decrease. Therefore, by comparing the ultrasonic velocity of liquid-nitrogen-cooled samples with that of naturally cooled samples, the further cracking effect of liquid-nitrogen cooling on high-temperature granite can be effectively analyzed based on heating damage. For example, if the ultrasonic velocity of a liquid-nitrogen-cooled sample is lower than that of a naturally cooled one at the same heating temperature, the damage degree of high-temperature granite is proven to have improved due to liquid-nitrogen cooling.

To better evaluate the effect of different cooling methods on the damage state of high-temperature granite, ultrasonic velocity was tested on the high-temperature granite with natural cooling and liquid-nitrogen cooling, and the change rules were compared. As shown in Figure 5, the ultrasonic velocity of both naturally cooled and liquid-nitrogen-cooled samples showed a significant decreasing trend with the increase in heating temperature. Among them, the ultrasonic velocity of the liquid-nitrogen-cooled sample at the same heating temperature was lower than that of the naturally cooled sample, which indicated that the damage degree caused by liquid-nitrogen cooling to the high-temperature granite was greater than that of natural cooling. Furthermore, liquid-nitrogen cooling can increase the internal microcrack volume of high-temperature granite. Since the heating processes of the naturally cooled and liquid-nitrogen-cooled samples were the same, the thermal damage caused by the heating process was almost the same. However, for the liquid-nitrogen-cooled samples, the cryogenic damage caused by liquid nitrogen was equivalent to that caused by thermal damage, which further increased the internal damage to the sample. Therefore, the ultrasonic velocity of the liquid-nitrogen-cooled sample was lower than that of the naturally cooled sample at the same heating temperature.

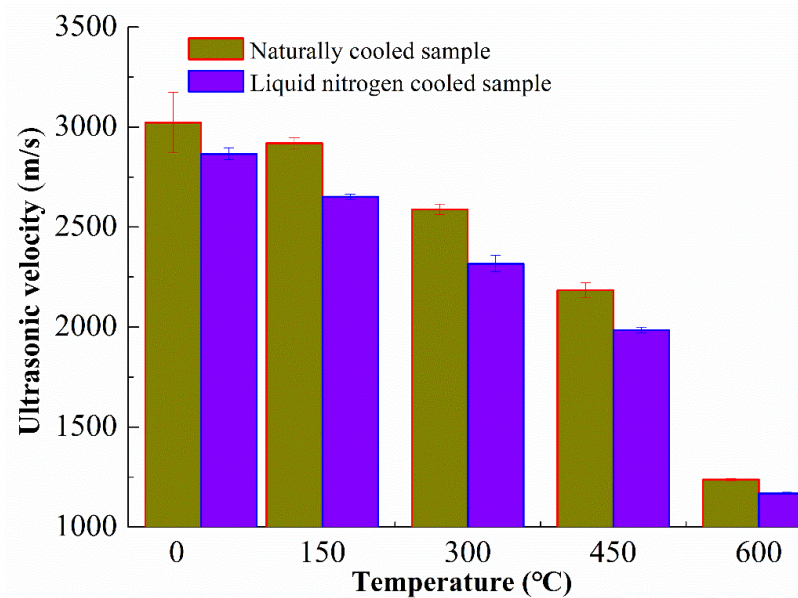


Figure 5. Characteristics of the ultrasonic velocity change caused by different cooling methods for high-temperature granite.

3.2. Deformation and Strength Characteristics

3.2.1. Change Law of Tensile Strength

As shown in Figure 6, both naturally cooled and liquid-nitrogen-cooled samples broke down along the center of the disc in the Brazilian splitting tests, and the cracking direction was consistent with the loading direction. This is a typical tensile failure. To better evaluate the effect of liquid-nitrogen cooling on rock tensile failure, a comparative analysis of tensile strength was carried out. Tensile strength is an important parameter to describe the ability of a rock to resist tension failure. During the Brazilian splitting tests of the naturally cooled and liquid-nitrogen-cooled samples, tensile strength changed due to the heating and cooling processes. By comparing the change characteristics of tensile strength under different cooling methods at the same heating temperatures, the influence of liquid nitrogen at low temperatures on the tensile strength of high-temperature granite can be effectively evaluated.

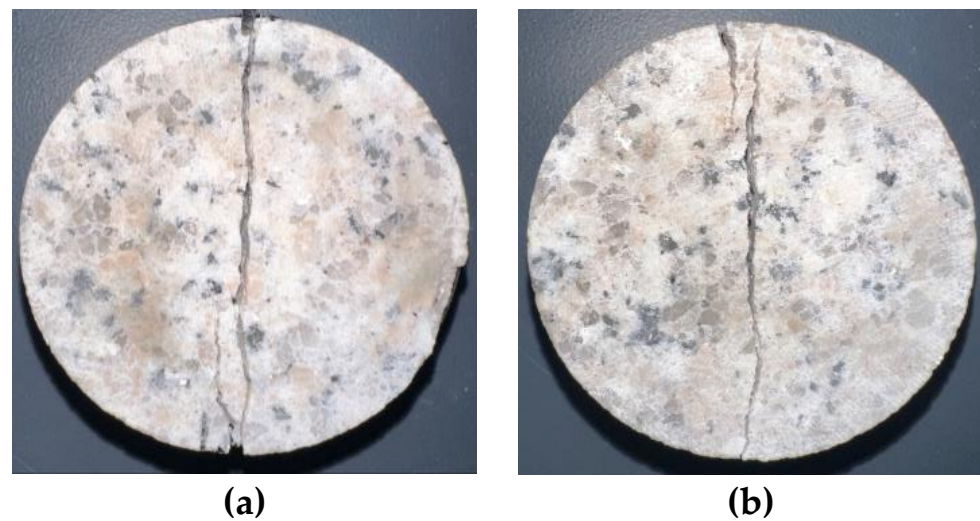


Figure 6. The failure form of naturally cooled and liquid-nitrogen-cooled samples in Brazilian splitting tests: (a) naturally cooled sample 150-A-1[#]; (b) Liquid-nitrogen-cooled sample 150-L-1[#].

After the Brazilian splitting test, the tensile strength values of the different samples were calculated according to the size parameters and the peak load. The results are shown in Figure 7. The tensile strength of granite was significantly affected by the heating temperature. In particular, when the heating temperature exceeded 300 °C, the tensile strength decreased significantly with the increase in temperature. For example, when the heating temperature was below 300 °C, the tensile strength of the naturally cooled sample was 13.18~14.12 MPa. However, when the heating temperature was above 450 °C, the tensile strength of naturally cooled samples decreased to 3.36~8.78 MPa. This indicated that, in the preparation of granite samples, heat treatment caused microcracks to form inside the granite and led to the deterioration of mechanical properties. Therefore, the influence of the heating process cannot be ignored when analyzing the influence of liquid-nitrogen cooling on the mechanical strength of high-temperature granite. By comparing the tensile strength of the naturally cooled sample with the liquid-nitrogen-cooled sample, the tensile strength of the liquid-nitrogen-cooled sample was always lower at the same heating temperature. This indicates that liquid-nitrogen cooling can aggravate the deterioration of the mechanical properties of high-temperature granite. In the test, the tensile strength of liquid-nitrogen-cooled rock samples was 5.96~26.40% lower than that of naturally cooled samples. This was mainly because liquid-nitrogen cooling formed a greater temperature gradient in the high-temperature granite, resulting in higher thermal stress and more microcracks. In addition, with the increase of heating temperature, the tensile strength of naturally cooled and liquid-nitrogen-cooled samples became increasingly closer in value, indicating that the deterioration of liquid-nitrogen cooling on the mechanical strength of high-temperature granite decreases with the increase in rock temperature, and the deterioration of the mechanical strength of high-temperature granite is mainly affected by the heating process.

3.2.2. Change in Splitting Modulus

The splitting modulus is an important parameter to evaluate rock deformation characteristics during the tensile failure process, which reflects the ability of a rock to resist compression deformation in the process of tensile failure. In general, the larger the splitting modulus of the rock, the smaller the compression displacement of the rock during the Brazilian splitting test. When the rock produces new fractures under the action of external load or temperature, the number of microfissures in the rock increases. The stiffness of the crack surface is less than that of the rock, which leads to a larger displacement of the rock under the same load increment. As a result, the splitting modulus of rock decreases.

Therefore, in this work, splitting modulus was employed to evaluate the evolution of rock mechanical properties under liquid-nitrogen cooling. There are three calculation methods [28]: (1) paste the strain gauge in the center of the disk sample to test the strain value perpendicular to the loading direction; (2) Establish the relationship between the displacement and the load perpendicular to the loading direction; (3) The load–displacement curve in the Brazilian splitting test is transformed into a stress–strain curve. The load is divided by the meridional area of the disk sample, and the displacement is divided by the diameter of the sample. The shape of the transformed curve is completely consistent with that of the load–displacement curve, and the slope of the straight-line section of the transformed curve is the splitting modulus. In this work, the third method was chosen, and the calculated results are shown in Figure 8.

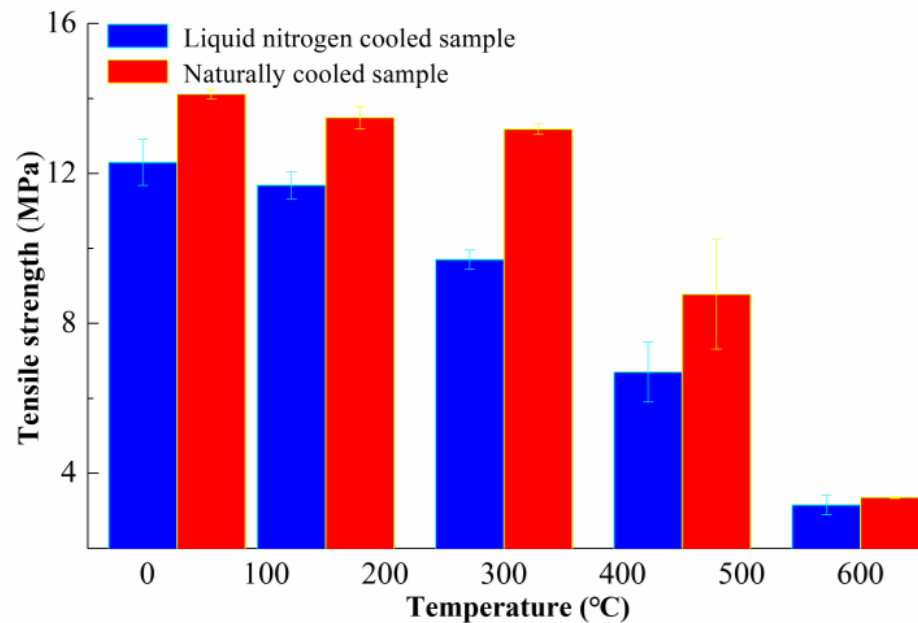


Figure 7. Tensile strength of granite under different heating and cooling modes.

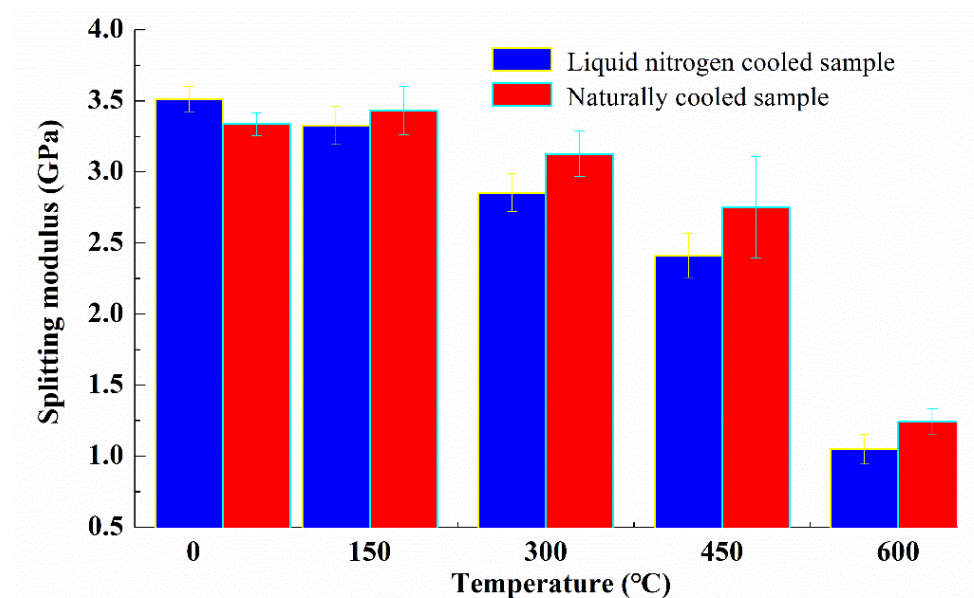


Figure 8. Relationship of splitting modulus of high-temperature granite with heating temperature under different cooling methods.

Figure 8 shows that with the increase in heating temperature, the splitting modulus of the granite generally decreases after cooling, which indicates that the heating process weakens the ability of the granite to resist elastic deformation. In this case, the large deformation of the granite occurred at a lower load. For example, when the heating temperature increased to 600 °C, the splitting modulus of the naturally cooled rock sample was only 37.24% of the initial state. This shows that resistance to the deformation of granite was greatly reduced during loading. For a heating temperature ranging from 25 to 600 °C, the splitting modulus of the liquid-nitrogen-cooled sample was generally lower than that of the naturally cooled sample at the same heating temperature. In particular, when the heating temperature exceeded 150 °C, the splitting modulus of the liquid-nitrogen-cooled sample was 3.01~15.53% lower than that of the naturally cooled sample at the same heating temperature. In addition, the difference between them also increased with the increase in heating temperature. In conclusion, after liquid-nitrogen cooling, not only is the tensile strength of high-temperature granite decreased, but also its resistance to deformation is further decreased. This helps reduce the elastic deformation of granite during loading and promotes the propagation of internal microcracks. The liquid-nitrogen-cooled sample was directly cooled to the liquid-nitrogen temperature from the heating temperature. Under the condition of heating, the sample was in a state of expansion, and the higher the heating temperature, the greater the thermal expansion of the rock sample. When the high-temperature sample was cooled in liquid nitrogen, the rock sample changed from an expansion state to a shrinkage state, resulting in greater shrinkage deformation and thermal stress. When the thermal stress in some areas exceeded the yield strength of the rock sample, there was plastic deformation, which made the rock sample more compact and more rigid. Therefore, in the subsequent loading process, the elastic deformation of the rock samples treated by liquid-nitrogen cooling was reduced to a certain extent.

3.2.3. Analysis of the Cooling Effect

To better characterize the influence of liquid nitrogen on the mechanical properties of high-temperature granite, the cooling effect coefficient $\lambda(T)$ at different heating temperatures must be defined. This coefficient represents the reduction of the relevant physical property parameters of granite at different heating temperatures compared with the initial state. The specific expression is as follows:

$$\lambda(T) = 1 - \frac{I(T)}{I(25)} \quad (1)$$

where $I(T)$ is the physical property parameters of granite under different heating temperatures, and $I(25)$ is the physical property parameters in the initial state (i.e., the temperature is 25 °C). The selected parameters comprise ultrasonic velocity, tensile strength, splitting modulus, etc.

The relationships between the cooling effect coefficient and the heating temperature of the liquid-nitrogen-cooled sample and the naturally cooled sample were calculated according to Equation (1). As shown in Figure 9, the cooling effect coefficient of liquid-nitrogen-cooled and naturally cooled samples increases as the heating temperature increases. The cooling effect coefficients calculated based on ultrasonic velocity and tensile strength are closely related to the cooling method. The cooling effect coefficient of the liquid-nitrogen-cooled samples was greater than that of naturally cooled rock samples at the same heating temperature, and the difference between the two rock samples first increased and then decreased with the increase in heating temperature. This shows that when the heating temperature exceeds a certain degree, the cooling effect of liquid nitrogen on high-temperature granite begins to weaken, and the influence of damage caused by heating on its mechanical properties plays a dominant role.

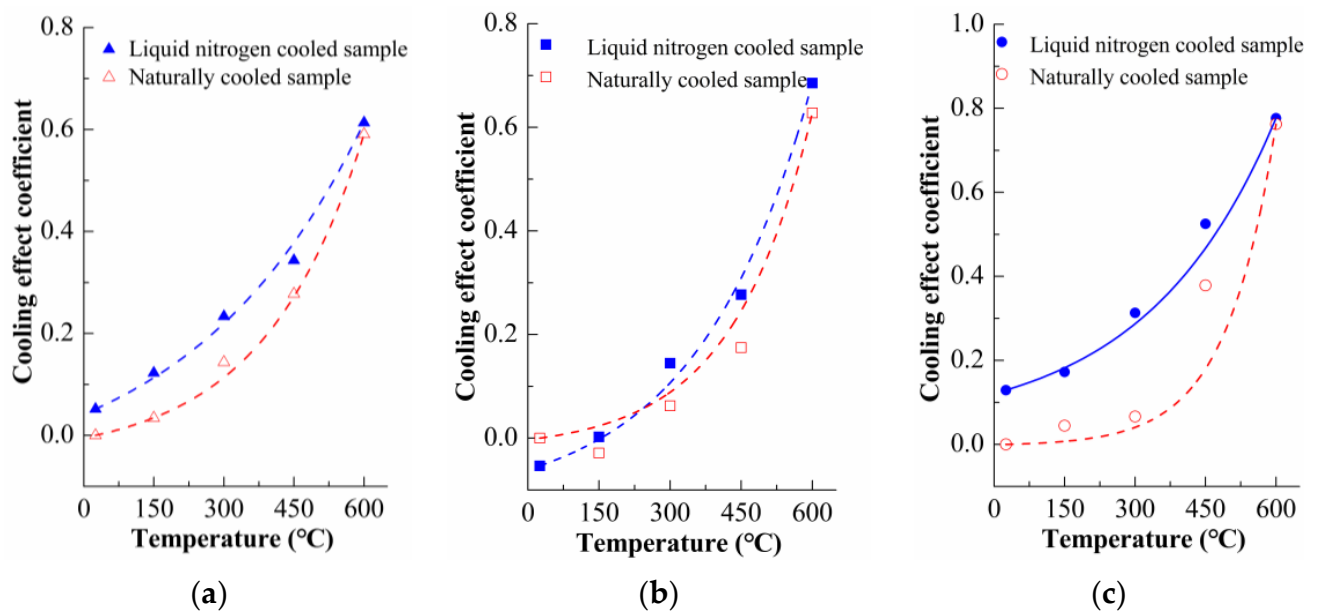


Figure 9. Cooling effect coefficient caused by different cooling modes: (a) calculated based on ultrasonic velocity; (b) calculated based on splitting modulus; (c) calculated based on tensile strength.

3.3. Characteristics of the AE Parameters

As a natural material, rock contains many internal defects. Under the action of external force or temperature load, these defects will continue to expand and nucleate, forming local damage and resulting in the AE phenomenon. This phenomenon can be used to analyze the damage characteristics and internal structure variation of rock in the loading process. Therefore, it is necessary to acquire and analyze the corresponding AE signals in the loading process, and then conduct damage assessment according to the characteristic parameters. First, the monitored signals are preprocessed and converted into different AE characteristic parameters. Then, statistical analysis is completed according to the variation rule of these characteristic parameters. The AE phenomenon is closely related to the damage evolution process inside the rock [29]. In this work, the ring-down count parameters in the loading process of the rock were used for analysis. AE ring-down count refers to the number of oscillations exceeding the threshold voltage, which is divided into the total number and the count rate, mainly reflecting the frequency and intensity of AE signals. This can be used to evaluate the activity of AE phenomena.

3.3.1. AE Parameters Characteristics for Granite Deformation and Failure

Figure 10 shows the typical AE ring-down count curve of heated granite in the process of the Brazilian splitting test. Although the test process was short and the sample failed rapidly, many AE signals were still detected during the deformation and failure process. At the initial stage of loading, AE ring-down count points were very sparse, and the cumulative ring-down count curve increased slowly with time. When the load increased to a certain extent, AE ring-down count points became denser, and the cumulative ring-down count curve increased abruptly. When the AE cumulative ring-down count curve increased abruptly, the AE ring-down count increased steadily, and at this time, the cumulative ring-down count-time curve was approximately a straight line. When the rock sample split, the AE ring-down count curve spiked again, and many AE signals were detected over a short time.

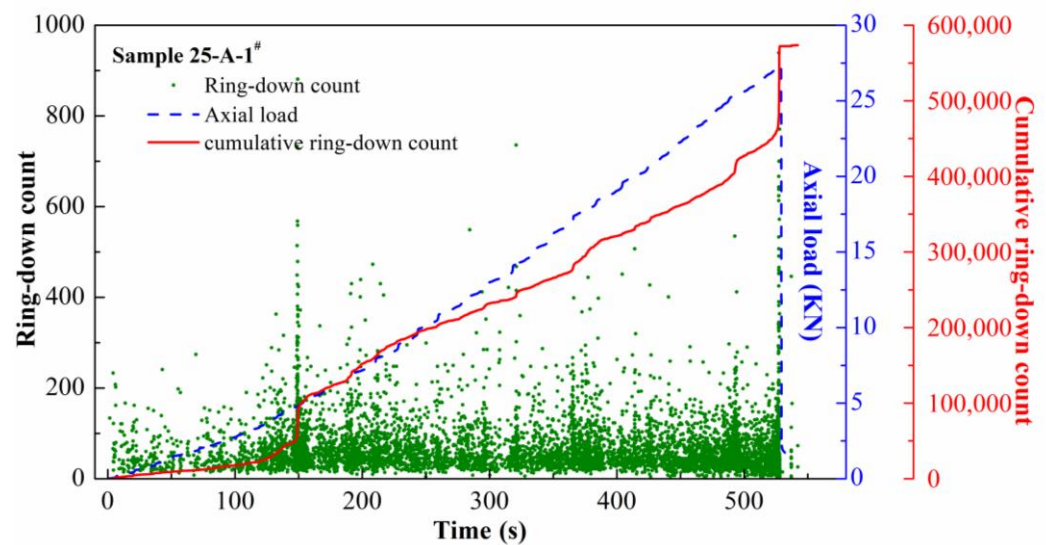


Figure 10. AE ring-down count curve of heated granite during the Brazilian splitting test.

To better analyze the effect of liquid-nitrogen cooling on the failure process of high-temperature granite, the cumulative ring-down count ratios at different load-ratio intervals were calculated. The cumulative ring-down count ratio shows the ratio of total AE ring-down counts in each load interval to total AE ring-down counts in the failure process. Taking 10% of the peak load as the range of variation, the statistical results of the AE ring-down count ratio in the failure process of naturally cooled and liquid-nitrogen-cooled samples were obtained. As shown in Figure 11, the AE signals monitored during the test were mainly concentrated at the time of failure, i.e., in a load interval of 90~100%. However, for high-temperature granite with different heating temperatures, the ring-down count ratios were significantly affected by liquid-nitrogen cooling at different load-ratio intervals. When the heating temperature was low, especially below 150 °C, the AE activity of the naturally cooled samples was very low in the low load interval (load level below 30~40%). For example, for samples with an initial temperature of 25 °C, when the load ratio exceeded 30%, there was an obvious AE phenomenon in the naturally cooled samples during loading. When the heating temperature was 150 °C, although the cumulative ring-down count ratio of the naturally cooled rock sample in the low load interval was higher than that of the naturally cooled sample with 25 °C, the AE activity level remained at a low level. For example, at 0~10%, 10~20%, and 20~30% load intervals, the cumulative AE ringing count ratios were only 1.04%, 4.58%, and 2.25%, respectively. However, when samples that were heated to 25 °C and 150 °C were cooled using liquid nitrogen, the AE activity of liquid-nitrogen-cooled samples at low load intervals was significantly improved, and the AE ring-down count ratio reached a higher level even in the load-ratio interval of 0~10%. For samples that were heated to 25 °C and 150 °C, the AE ring-down count ratio of liquid-nitrogen-cooled samples in the 0~10% load-ratio interval reached 18.06% and 23.72%, respectively, which is consistent with the AE ring-down count ratio at the 70~80% load-ratio interval. It can be seen that liquid-nitrogen cooling can significantly increase the damage degree of high-temperature granite, promote the growth of microcracks, and make microcracks fully expand under low load levels after liquid-nitrogen cooling. Therefore, many AE signals can be monitored. From a mesoscopic perspective, the failure of rock is caused by local fracture zones formed by the propagation and interaction of internal microcracks. Therefore, the greater the number of microcracks in the rock, the easier it is for the microcracks to interact with one another in the process of propagation. This makes it easier for the rock to enter the stage of unstable crack propagation in the process of loading. According to the ultrasonic test results, the number of internal microcracks in high-temperature granite further increased after liquid-nitrogen cooling. This was equivalent to the initial degree

of damage inflicted on the liquid-nitrogen-cooled sample before loading, suggesting that the rock could enter the crack instability stage propagation at a low load level.

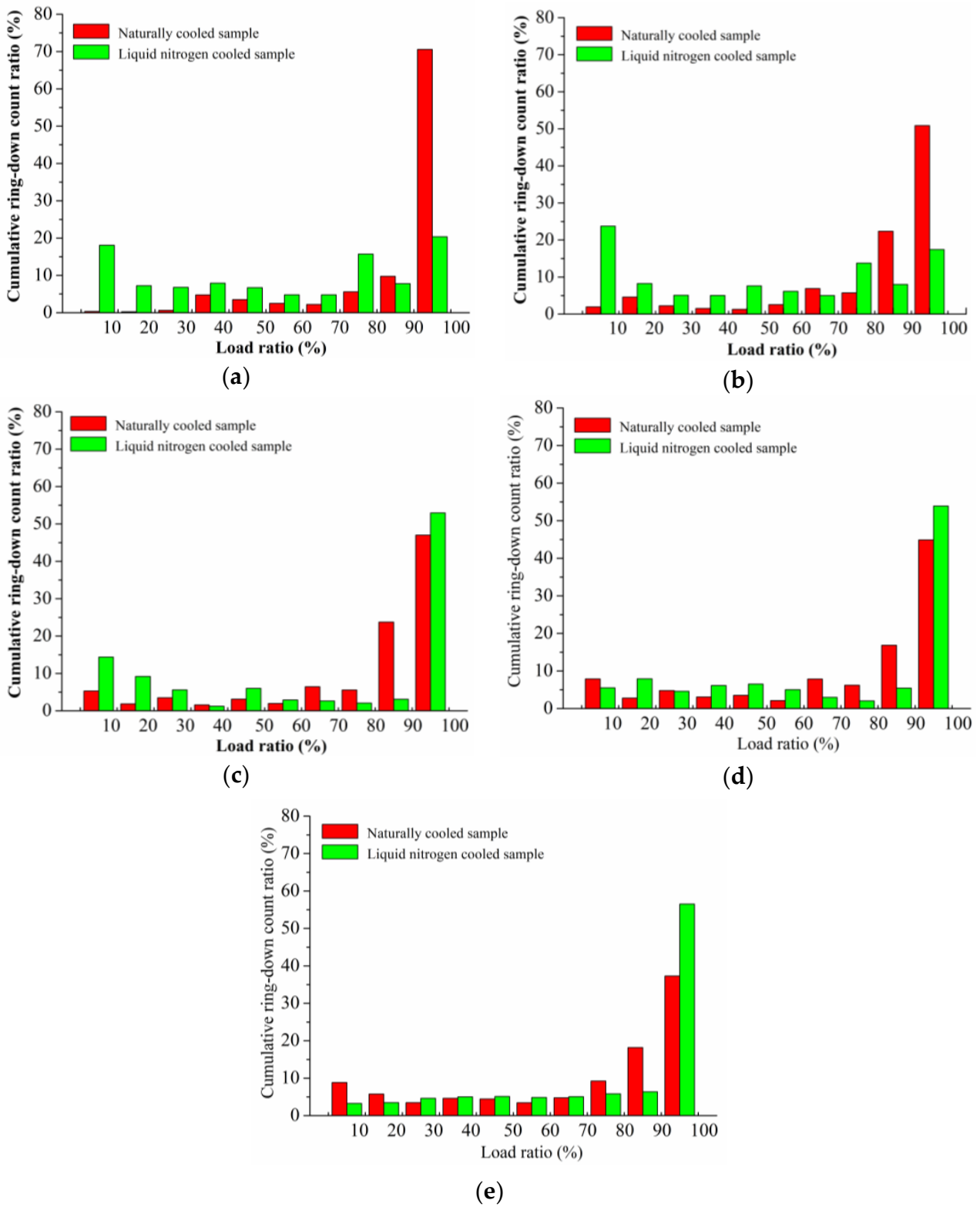


Figure 11. Cumulative AE ring-down count ratio of naturally cooled and liquid-nitrogen-cooled samples in the process of failure at different load-ratio intervals: (a) 25 °C; (b) 150 °C; (c) 300 °C; (d) 450 °C; (e) 600 °C.

With an increase in heating temperature, the ring-down count ratio of the naturally cooled samples at a low load-ratio increases. In the initial loading stage (load ratio of less than 10%), the AE signal in the granite sample was mainly produced by the closure of microcracks. Because the granite was very dense and the number of microcracks was very small, the AE signal of granite was less in the initial loading stage at room temperature. Therefore, as shown in Figure 11a, when the load ratio was less than 10%, there was almost no AE ringing signal detected in the naturally cooled sample at 25 °C. However, with the continuous increase in heating temperature, the number of AE signals in the naturally cooled samples increased steadily in the initial stage, which also indicates that the heating process can indeed increase the number of microfissures in granite. As a result, there were more microcracks closed in the naturally cooled samples at the initial loading stage, so the ring-down count ratio increased accordingly. For example, when the load-ratio interval was in the range of 0~10%, the ring-down count ratios of the naturally cooled samples with 25 °C, 150 °C, 300 °C, 450 °C, and 600 °C heating temperatures were 0.31%, 0.94%, 5.29%, 7.88%, and 8.83%, respectively, indicating that the AE activity increased steadily with the increase of heating temperature at the initial loading stage. This indicates that as the temperature of high-temperature granite increases, the number and size of microcracks in the sample increase, and this can generate AE signals at low loading levels. Due to the enhanced AE activity during the loading process, the ring-down count ratios of the naturally cooled samples near the failure decreased with the increase in temperature. For example, when the heating temperature increased from 25 °C to 600 °C, the AE ring-down count ratio of the naturally cooled samples in the load-ratio interval of 90~100% decreased from 70.57% to 37.29%.

Compared with the naturally cooled samples, the ring-down count of the liquid-nitrogen-cooled rock samples presented a more complex variation trend with the load ratio. For example, when the heating temperature was low (below 300 °C), the liquid-nitrogen cooling significantly increased the AE activity of high-temperature granite at a low load ratio. Therefore, obvious AE activity was detected in liquid-nitrogen-cooled samples at each load level stage, i.e., there was no obvious AE silence period observed in liquid-nitrogen-cooled samples. In particular, when the load ratio was below 30%, the ring-down count ratio of the liquid-nitrogen-cooled samples was higher than that of the naturally cooled samples under the same load ratio. However, as the heating temperature continued to rise (>300 °C), the ring-down count ratio of the liquid-nitrogen-cooled sample at a low load-ratio interval began to decrease. For example, when the heating temperature reached 450 °C and 600 °C, the ring-down count ratio of the liquid-nitrogen-cooled sample was significantly higher than that of the naturally cooled sample, not only in the range of the 0~10% load-ratio interval but also in the range of the 90~100% load-ratio interval. This indicates that when the heating temperature reaches a certain level, the proportion of AE signals detected in liquid-nitrogen-cooled samples decreases at a low load level, while that detected at a high load level increases. This is mainly because the AE phenomenon of rock materials in the loading process displays the Kaiser effect. When the load level of the rock exceeds the previous maximum stress level, AE signals will be detected again. Due to the extremely low temperature, when liquid nitrogen is used to cool high-temperature granite, huge thermal stress inside the high-temperature granite is generated. The thermal stress value even exceeds the stress value in the early loading stage of the Brazilian splitting test. Thus, compared with the naturally cooled method, liquid-nitrogen cooling can produce a stronger cooling impact effect in high-temperature granite, making the high-temperature granite bear greater thermal stress before loading. This could effectively increase the deterioration degree of the mechanical properties of high-temperature granite. Consequently, the ultrasonic velocity and tensile strength of the liquid-nitrogen-cooled sample are lower than that of the naturally cooled sample at the same heating temperature.

3.3.2. The Influence of Liquid-Nitrogen Cooling on the Failure of High-Temperature Granite

To further evaluate the effect of liquid-nitrogen cooling on the failure process of high-temperature granite, the relationship between the normalized cumulative ring-down count and the load ratio of naturally cooled and liquid-nitrogen-cooled samples during the loading process was statistically analyzed. The normalized cumulative ring-down count in this work is defined as the ratio of the cumulative AE ring-down count at the corresponding load ratio to the total cumulative AE ring-down count at the peak load. The statistical results are shown in Figure 12. As shown in this figure, the AE signals of naturally cooled and liquid-nitrogen-cooled samples increased with the growth of the load ratio. When the load ratio is less than 80%, the normalized ring-down count of the naturally cooled sample increases slowly with the increase of the load ratio. When the load ratio increases from 80% to 100%, the normalized ring-down count increases rapidly. Taking a naturally cooled sample with 150 °C heating temperature as an example, when the load ratio increased from 80% to 100%, the normalized cumulative ring-down count increased from 0.27 to 1, indicating an increase of 270.37%. However, when the load ratio increased from 40% to 80%, the normalized cumulative ring-down count increased from 0.10 to 0.27, presenting an increase of 170%. It can be seen that although the AE signals of naturally cooled samples increased under a low load ratio due to heating treatment, AE signals were still concentrated at the peak load stage, i.e., the propagation of microcracks was mainly concentrated at the failure moment. In addition, for the same load ratio, the normalized cumulative ring-down count of naturally cooled samples increased with the increase in heating temperature. Taking the loading ratio of 40% as an example, when the heating temperature increased from 25 °C to 600 °C, the normalized cumulative ring-down count increased from 0.06 to 0.23, with an increase of 283.33%. This indicates that with the increase in heating temperature, the propagation of microcracks inside the sample is promoted, and it is easier to generate more AE signals at a low load ratio.

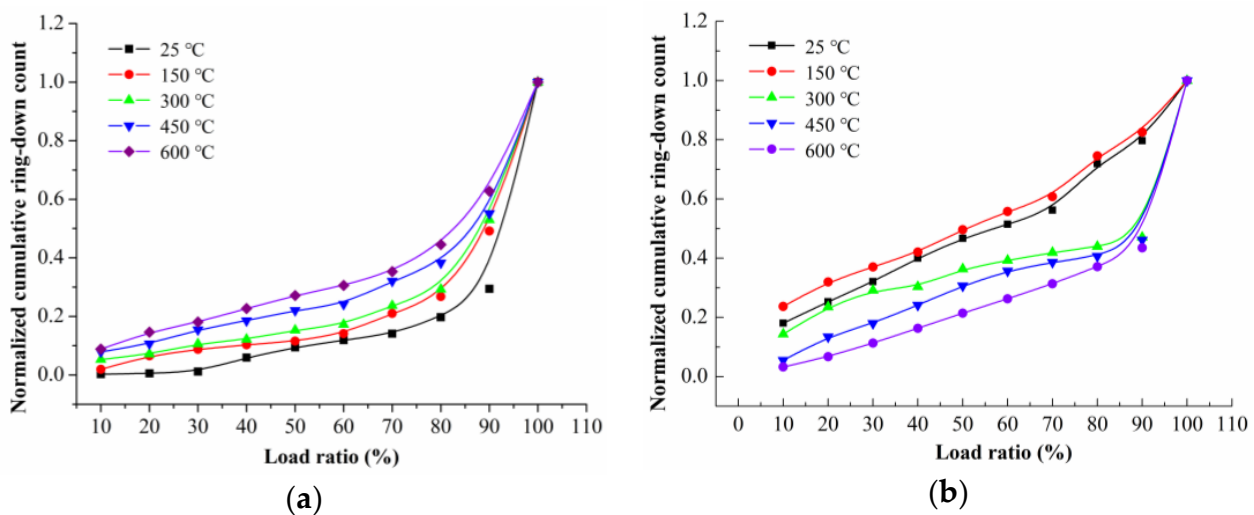


Figure 12. Relationship of normalized cumulative ring-down count and load ratio: (a) naturally cooled sample; (b) liquid-nitrogen-cooled sample.

For the liquid-nitrogen-cooled samples, the trend of normalized cumulative ring-down count varied significantly with load ratio. For example, when the heating temperature was 25 °C and 150 °C, the normalized cumulative ring-down count showed a steady growth trend with the increase of the load ratio, and there was no sudden increase in the normalized cumulative ring-down count near the peak load. Similarly, taking the liquid-nitrogen-cooled sample with 150 °C heating temperature as an example, when the load ratio increased from 80% to 100%, the normalized ring-down count increased from 0.75 to 1, with an increase of only 25%. This was much smaller than that of the naturally cooled sample at the same heating temperature. When the load ratio increased from 40%

to 80%, the normalized ring-down count increased from 0.42 to 0.75, with an increase of 78.57%, which was still smaller than that of the naturally cooled sample. It can be seen that liquid-nitrogen cooling promoted the expansion of microcracks in high-temperature granite at each loading stage. This helps improve the fracture uniformity of samples during loading. However, at the same loading ratio, the normalized cumulative ring-down count of the liquid-nitrogen-cooled samples increased first and then decreased with the increase in the heating temperature. In particular, when the heating temperature exceeded 300 °C, the AE signals of liquid-nitrogen-cooled samples showed a sudden increasing trend near the peak load.

To further analyze the effect of liquid-nitrogen cooling on the failure process of high-temperature granite, referring to the method proposed by Liu [30], the ratio of the cumulative AE ring-down count within the range of the 80–100% load-ratio interval to the cumulative AE ring-down count in the whole loading stage is defined as the peak ring-down count ratio. This value can be used to characterize the severity of rock failure at the peak loading stage. As shown in Figure 13, the peak ring-down count ratio of the naturally cooled sample decreased as the heating temperature increased. For example, when the heating temperature increased from 25 °C to 600 °C, the peak ring-down count ratio decreased from 0.80 to 0.55, presenting a decrease of 31.25%. This indicates that with the increase in heating temperature, the damage severity of the naturally cooled sample at the peak load decreases. For the liquid-nitrogen-cooled sample, the peak ring-down count ratio increases with the increase in heating temperature. For example, when the heating temperature increased from 25 °C to 600 °C, the peak ring-down count ratio increased by 125% from 0.28 to 0.63. This was mainly because, compared with the natural cooling method, liquid-nitrogen cooling can generate greater thermal stress inside the high-temperature granite, so the high-temperature granite is subjected to greater thermal stress before loading. Under the influence of the AE Kaiser effect, the level of AE signals generated in the liquid-nitrogen-cooled sample is low at a low load ratio. Only when the load ratio reached a certain degree (exceeding the thermal stress generated by liquid-nitrogen cooling), the expansion of microcracks in the sample can produce obvious AE signals. This also indirectly proves that liquid-nitrogen cooling can further increase the damage degree of high-temperature granite, leading to a further reduction of mechanical properties.

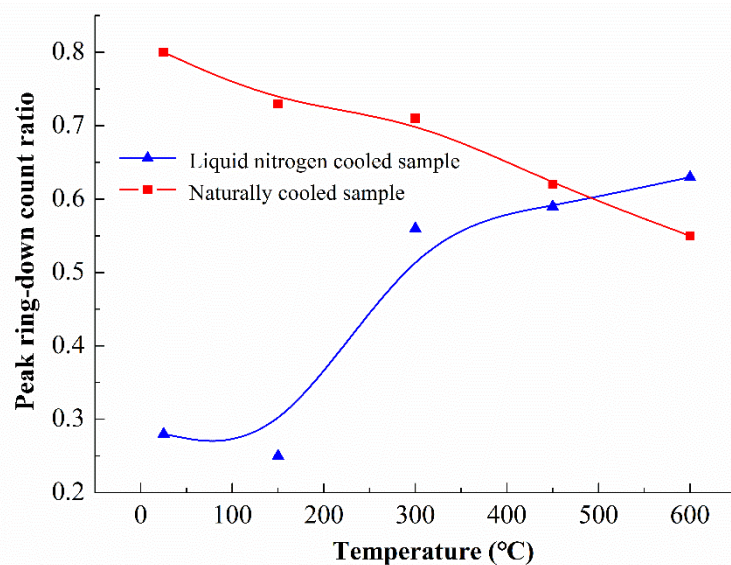


Figure 13. Peak ring-down count ratio of naturally cooled and liquid-nitrogen-cooled samples at different heating temperatures.

3.4. Characteristics of the Energy Evolution

3.4.1. Energy Evolution Mechanism during Rock Loading

The law of energy evolution is an important way of studying rock deformation and failure characteristics and has been widely used in rock mechanics analysis and testing [31]. Compared with the traditional stress method, this method analyzes the deformation and failure process of rock from the perspective of energy, which is closer to the essence of rock failure [31]. Load displacement, as a description of a specific mechanical state, is only a performance of a certain aspect of the thermodynamic state of rock, and cannot reflect the essential physical characteristics of rock. According to the law of thermodynamics, energy transformation is the essential characteristic of a material physical process, and the failure of rock is an unstable phenomenon driven by energy. The dynamic failure of rock is the result of a sharp release of elastic deformation energy accumulated when the strength limit is reached. Therefore, the law of energy evolution in the process of rock deformation and failure can be analyzed in detail, and the failure theory based on energy change can be established. It is expected to truly reflect the failure law of rock and better serve relevant engineering practices.

From the microscopic perspective, rock deformation and failure are the result of internal damage evolution, which is caused by the continuous expansion of initial defects such as microcracks. In the process of microcrack expansion, energy is absorbed to produce new crack surfaces. This means that some of the work done to the rock by external forces (i.e., the energy absorbed by the rock) is dissipated in the form of microcracks, and this energy is called dissipated energy. In addition to dissipated energy, another part of the energy absorbed by the rock is stored inside the rock in the form of elastic deformation, which is called elastic energy. Xie et al. [32] pointed out that dissipated energy leads to the continuous expansion of internal defects and the deterioration of the mechanical properties of rock, and ultimately to the loss of rock strength, which is the essential property of rock failure. For the same type of rock, the law of energy evolution is mainly affected by the initial microcrack distribution in the rock. This is because the initial microcrack distribution affects the energy dissipation process of the rock such that the energy dissipation law of the rock presents different characteristics. This is also the basis for evaluating the damage characteristics of rock according to energy evolution.

There is a lot of energy involved in the rock loading process, so it is impossible to monitor every kind of energy during the experiment. In the analysis of rock deformation and failure, elastic energy and dissipated energy are mainly studied. If the heat exchange between the rock and the outside environment is ignored, the energy absorbed by the rock can be regarded as the sum of elastic energy and dissipated energy according to the first law of thermodynamics:

$$U = U^e + U^d \quad (2)$$

where U is the work done on the rock by external forces, i.e., absorbed energy; U^e is the elastic energy stored inside the rock; and U^d is the dissipated energy of the rock.

The calculation of elastic energy, dissipated energy, and absorbed energy can be made according to the method provided in the literature [33].

3.4.2. The Influence Law of Liquid-Nitrogen Cooling on Energy Evolution

From the perspective of thermodynamics, microcrack propagation is a process of energy consumption. In the Brazilian splitting test, the energy absorbed by the rock is mainly from the work done to the rock by external forces. Part of this energy is stored in the form of elastic energy, and the other part is mainly dissipated to promote the expansion of microcracks. This can be seen from the load–displacement curve of the samples (Figure 14), where both natural cooling and liquid-nitrogen cooling affected the load–displacement curve of high-temperature granite, and the curve changed mainly in the form of peak load decreasing with the growth of heating temperature. Among them, the peak load of the liquid-nitrogen-cooled sample was smaller than that of the naturally cooled sample under the same heating temperature. However, there was no obvious plastic deformation stage

before the failure of both the naturally and liquid-nitrogen-cooled samples. This indicates that the main form of energy dissipation is the generation of new damage. Therefore, the damage state and failure characteristics of rock could be analyzed and evaluated according to the law of energy evolution.

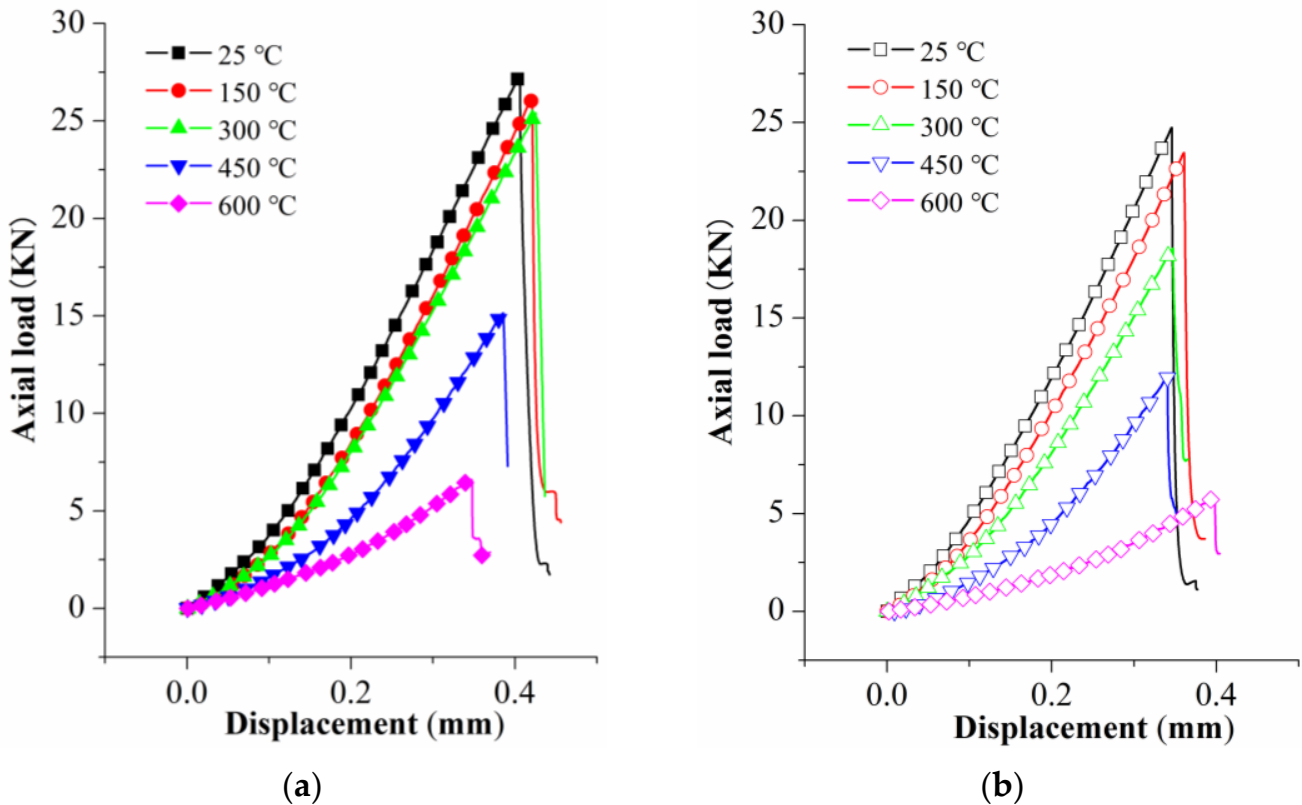


Figure 14. Load–displacement curves of naturally and liquid-nitrogen-cooled samples at different heating temperatures: (a) naturally cooled sample; (b) liquid-nitrogen-cooled sample.

- Effect on the elastic energy

In the process of energy evolution, elastic energy is stored in the form of elastic strain, so it is also called elastic strain energy, and its main role is to drive the rock to rupture [34]. The greater elastic energy during rock failure indicates that more elastic energy is required. Generally, the elastic energy of rock at the peak load is regarded as the energy storage limit of rock. The higher the energy storage limit of rock, the more complete the rock structure, and the better the mechanical properties of rock.

As shown in Figure 15, elastic energy showed a nonlinear growth trend with the increase in load ratio. At the beginning of loading, the growth rate of elastic energy was relatively slow. As the load ratio increased, the elastic energy increased increasingly quickly. When the heating temperature was lower than 450 °C, the elastic energy of the naturally cooled sample was always higher than that of the liquid-nitrogen-cooled sample under the same load ratio. This indicates that liquid-nitrogen cooling can further destroy the structural integrity of rock and reduce the energy storage limit. When the high-temperature granite (heating temperature ranging from ~25 to ~450 °C) was treated with liquid nitrogen, the maximum elastic energy decreased by 22.27~39.88%. For example, when the load ratio was 10%, the elastic energy of the naturally cooled sample was 22.45~39.18% higher than that of the liquid-nitrogen-cooled sample. When the load ratio was 80%, this value was up to 22.35~39.82%. It can be seen that the ability of high-temperature granite to store elastic energy is weakened after liquid-nitrogen cooling. This also proves that liquid-nitrogen cooling causes damage and cracking effects on high-temperature granite, which destroys its microstructure and degrades its mechanical properties. When the heating temperature

risers to 600 °C, due to the serious damage of granite in the heating process, the elastic energy of the naturally cooled sample was very close to that of the liquid-nitrogen-cooled sample. The difference between them was only 2.13–4.10%.

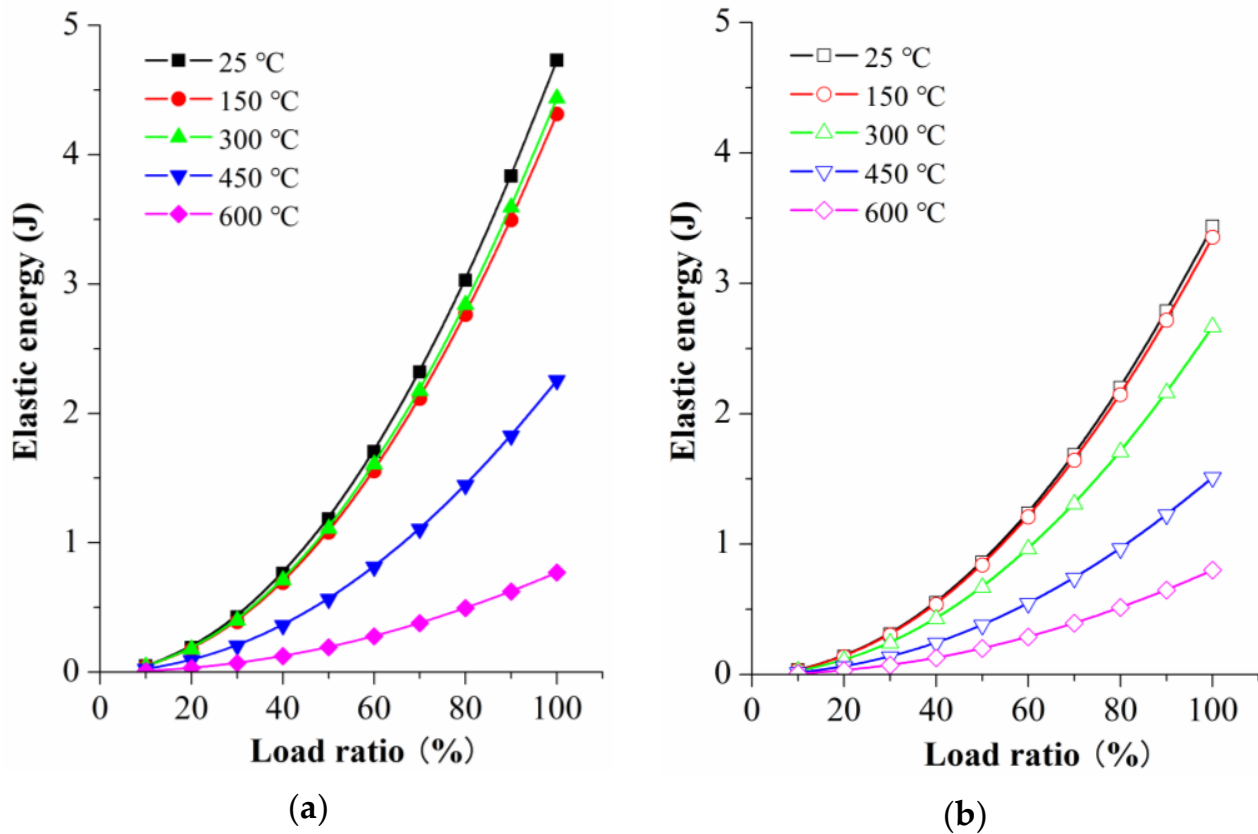


Figure 15. The curves of the elastic energy–load ratio of high-temperature granite under different cooling methods: (a) naturally cooled sample; (b) liquid-nitrogen-cooled sample.

- Effect on dissipated energy

In the loading process, the damage and plastic deformation of rock will cause energy dissipation. Energy dissipation can degrade the mechanical properties of rock, resulting in the reduction of cohesiveness between particles and the ability to resist damage. Therefore, energy dissipation is an essential property of rock failure, reflecting the continuous initiation, expansion, and interaction process of microcracks in rock [35]. The greater the dissipated energy during rock failure, the more energy there is that needs to be dissipated, which means that more microcracks need to be produced.

Figure 16 shows the relationship between dissipated energy and the load ratio of different samples in the loading process. The dissipated energy first increases and then decreases with the increase of the load ratio. For example, when the load ratio is low, the dissipated energy increases slowly with the increase of the load ratio. This is because the energy dissipation of the sample is mainly caused by the closure of microcracks at a low load ratio. With the increase in load, the internal microcracks of granite slowly close, causing the dissipated energy to decrease. At this time, the internal energy evolution of the sample is mainly dominated by the accumulation of elastic energy. In addition, with the increased heating temperature, the dissipated energy of the naturally and liquid-nitrogen-cooled samples increases first and then decreases with the increase of heating temperature. For example, when the heating temperature increases from 25 °C to 300 °C, the maximum dissipated energy of the naturally cooled samples increased from 0.23 J to 0.30 J with an increase of 30.43%; For the liquid-nitrogen-cooled samples, the maximum dissipated energy increased from 0.19 J to 0.28 J, with an increase of 47.37%. When the heating temperature

increased from 300 °C to 600 °C, the maximum dissipation energy of the naturally cooled sample decreased from 0.30 J to 0.15 J, with a decrease of 50%. However, for the liquid-nitrogen-cooled samples, the maximum dissipated energy decreased from 0.28 J to 0.16 J. This was mainly because when the heating temperature was low, natural cooling and liquid-nitrogen cooling led to an increase in microcracks of the high-temperature granite, and there was more energy that needed to be dissipated in the loading process of the rock sample to promote the closure of these microcracks. When the heating temperature reached a certain level, natural cooling and liquid-nitrogen cooling could significantly promote the deterioration of the mechanical properties of high-temperature granite, resulting in the reduction of the elastic modulus and other parameters. In this case, the granite samples presented large deformation under a low load ratio, and the microcracks were easier to close. As a result, the dissipated energy began to decrease with the continuous increase in heating temperature.

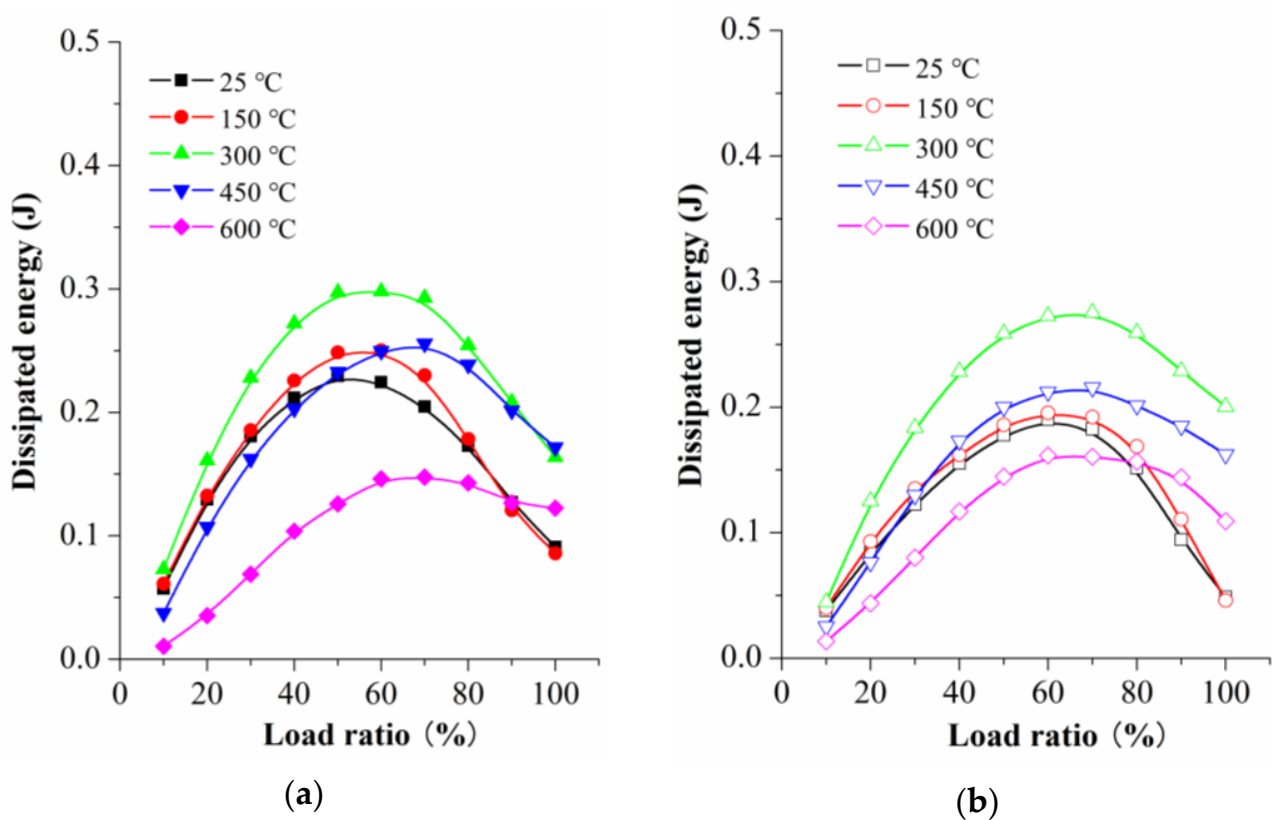


Figure 16. Dissipated energy–load ratio curves of high-temperature granite under different cooling methods: (a) naturally cooled sample; (b) liquid-nitrogen-cooled sample.

By comparing naturally cooled and liquid-nitrogen-cooled samples, it can be seen that under the same heating temperature, the dissipated energy of the naturally cooled samples was greater than that of the liquid-nitrogen-cooled samples. Compared with the naturally cooled samples (heating temperature of 25–450 °C), the peak dissipated energy of the liquid-nitrogen-cooled samples decreased by 15.72–34.41%. For example, when the heating temperature was 25 °C, 150 °C, 300 °C, 450 °C, and 600 °C, the maximum dissipated energy of the naturally cooled sample was 0.23 J, 0.25 J, 0.30 J, 0.26 J, and 0.15 J, respectively. In addition, the corresponding maximum dissipated energy of the liquid-nitrogen-cooled sample was 0.19 J, 0.20 J, 0.27 J, 0.22 J, and 0.16 J, respectively. This indicates that after liquid-nitrogen cooling, the energy dissipation of high-temperature granite reduces when it ruptures. This also means that the sample can be destroyed when fewer microcracks are additionally generated. It can be seen that liquid-nitrogen cooling made the microcracks in the high-temperature granite expand, increasing the number

of microcracks. Therefore, the number of newly generated microcracks and the energy dissipated in the liquid-nitrogen-cooled samples during the failure was smaller than that of the naturally cooled samples.

- Effect on the absorbed energy

Figure 17 shows the relationship between absorbed energy and the load ratio of the naturally cooled and liquid-nitrogen-cooled samples. The variation law of the absorbed energy with the load ratio is consistent with elastic energy. This is mainly because the elastic energy is much greater than the dissipated energy in the loading process, and the granite sample had no yield stage in the failure process. Therefore, elastic energy plays a major role in the evolution of energy. In addition, at the same load ratio and heating temperature, the absorbed energy of the liquid-nitrogen-cooled sample was less than that of naturally cooled rock. In particular, when the high-temperature granite (heating temperature in the range of 25~450 °C) was cooled with liquid nitrogen, the ultimate absorbed energy was reduced by 22.74~37.66%. For example, at the peak load, the absorbed energies of the liquid-nitrogen-cooled samples at 25 °C, 150 °C, 300 °C, 450 °C, and 600 °C were 4.82 J, 4.40 J, 4.60 J, 2.43 J, and 0.89 J, respectively. However, the absorbed energies of the naturally cooled samples were 3.49 J, 3.40 J, 2.87 J, 1.67 J, and 0.91 J, respectively. This indicates that the energy absorbed by high-temperature granite when a failure occurs is also greatly reduced after liquid-nitrogen cooling, and the failure of the granite sample is caused by less absorbed energy.

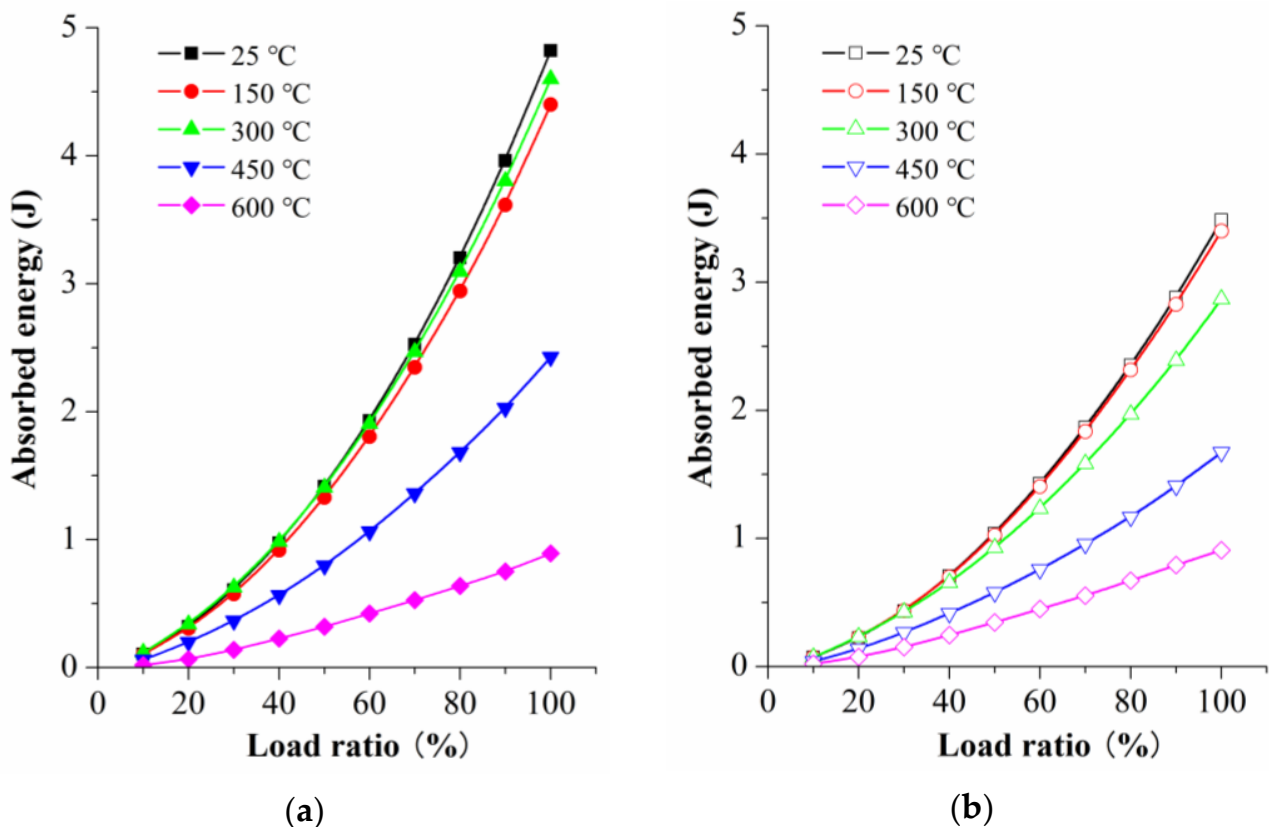


Figure 17. Curves of absorbed energy–load ratio of high-temperature granite under different cooling methods: (a) naturally cooled sample; (b) liquid-nitrogen-cooled sample.

- Effect on energy distribution

According to the above analysis, the energy absorbed by rocks has two main functions. First, it is stored in the form of elastic energy, which is used to drive rock failure. Second, it is dissipated in the form of new damage, which weakens the rock's ability to resist failure.

Therefore, it will be helpful to further understand the effect of liquid-nitrogen cooling on high-temperature granite by analyzing the energy distribution law in the loading process. Figure 18 shows the relationship between the energy proportions of naturally cooled and liquid-nitrogen-cooled samples and the load ratio. In contrast to the conventional axial compression test, the tensile strength of rock is far less than the compressive strength, and the load of the rock in the Brazilian splitting test is usually at a low level. At low load levels, rock does not easily produce elastic deformation. Because the stiffness of the crack is less than that of the rock, some of the microcracks will close along the normal direction of the crack surface. The closure of microcracks will consume energy. However, at a low load level, the elastic deformation of the rock was low, and the energy absorbed was mainly used for microcrack closure. Therefore, at the beginning of the Brazilian splitting test, the proportion of dissipated energy of the rock sample was larger than that of elastic energy.

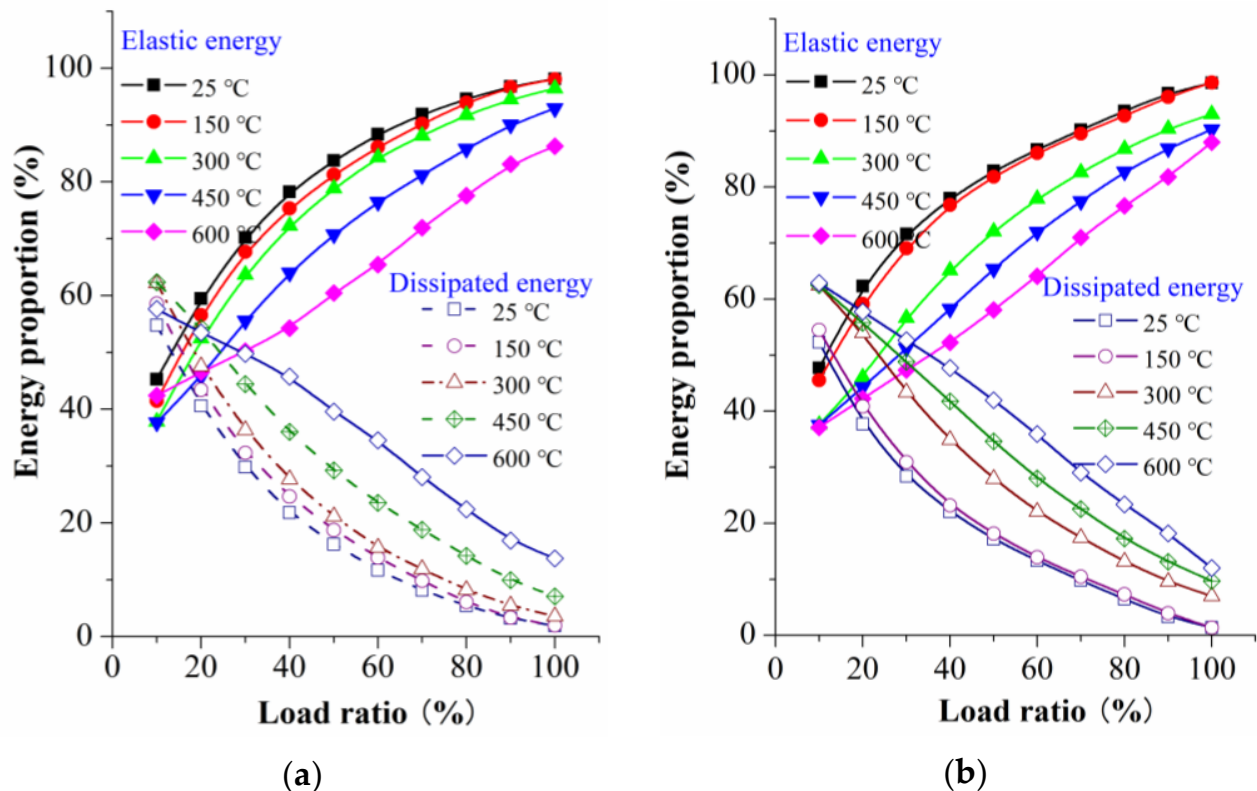


Figure 18. Relationship between the energy proportions and the load ratio: (a) naturally cooled sample; (b) liquid-nitrogen-cooled sample.

As shown in Figure 18, the proportions of elastic energy and dissipated energy in the loading process present changing trends with the increase in load ratio. The proportion of elastic energy increased steadily with the growth of the load ratio, while the proportion of dissipated energy decreased gradually. This indicates that, with the increase in load, the energy absorbed by the naturally cooled and liquid-nitrogen-cooled samples is mainly stored in the form of elastic energy, and dissipated energy is constantly reduced. The elastic deformation was dominant during the entire loading stage, which is consistent with the form of the load–displacement curve. Under the same load ratio, the proportion of elastic energy of the liquid-nitrogen-cooled samples was smaller than that of the naturally cooled samples, which indicates that the effect of liquid-nitrogen cooling helps to increase the damage inflicted on high-temperature granite and promotes the expansion of microcracks. Taking the 60% load ratio as an example, the elastic energy proportions of naturally cooled samples heated at 25 °C, 150 °C, 300 °C, 450 °C, and 600 °C were 88.36%, 86.13%, 84.34%, 76.47%, and 65.45%, respectively. Meanwhile, the elastic energy proportions of the liquid-nitrogen-cooled samples at the same heating temperature were 86.69%, 86.08%, 77.92%,

71.98%, and 64.08%, respectively. In conclusion, at a 60% loading ratio, liquid nitrogen cooling could further reduce the elastic energy proportion of the high-temperature granite by 0.06–7.61%.

4. Discussion

As a natural porous medium, rock contains many initial defects such as microcracks and micropores, which will significantly affect its physical and mechanical properties. According to damage mechanics theory, the greater the proportion of internal defects in rock, the higher the degree of damage. The essence of rock damage is the growth and expansion of microcracks, but these are difficult to measure and evaluate directly using experimental means. Macroscopically, rock damage is manifested as the deterioration of mechanical properties [34]. Therefore, the damage characteristics of rock can be evaluated by the change in its mechanical parameters.

The failure process of rock under external load is a process of initiation and continuous expansion of microcracks until nucleation. Microcracks in rock will have an impact on the failure characteristics of rock, i.e., on a macro level, rock damage can be characterized by the mechanical parameters of rock [32]. When liquid-nitrogen cooling produces a cracking effect on high-temperature granite, its mechanical parameters will change accordingly. Figure 19 is a schematic diagram of the sliding crack model commonly used to describe the crack penetration and nucleation theory of rock during loading [35]. The pre-existing crack represents an already-existing microcrack in the rock. When the shear stress of the pre-existing crack exceeds the friction force between crack surfaces, wing cracks will occur near the tip. The propagation and penetration of microcracks in the rock under the action of external forces are mainly caused by the continuous propagation of these wing cracks. Under the action of external force, these wing cracks further extend, expand, and connect. When the volume of wing cracks in the rock reaches a certain level, a local failure zone will form, resulting in fracture failure. For example, in refracturing technology, new turning fractures are produced at the tip of the original fractures, therefore increasing the volume of reservoir stimulation [36]. The more pre-existing cracks there are, the fewer new cracks will be required for rock failure, which means less energy will be consumed in the rock failure process. This is also the reason the dissipated energy of the liquid-nitrogen-cooled samples was less than that of the naturally cooled samples during the failure process.

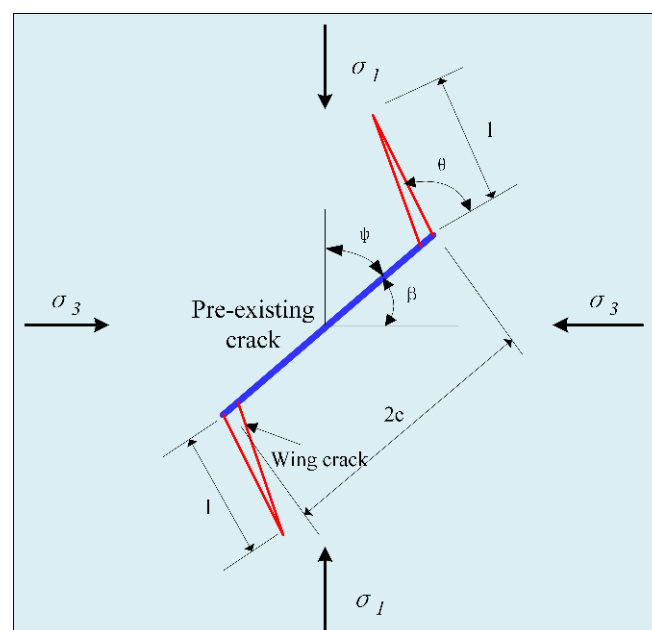


Figure 19. Sliding crack model.

5. Conclusions

In this paper, Brazilian splitting tests were carried out on granite at different heating temperatures and after different cooling treatments. The ultrasonic velocity, splitting modulus, tensile strength, energy evolution, and AE signal parameters were analyzed, and the following conclusions were obtained:

- (1) The ultrasonic velocity of high-temperature granite samples after both natural cooling and liquid-nitrogen cooling decreases with the increase in heating temperature. At each heating temperature, the ultrasonic velocity of the liquid-nitrogen-cooled samples was lower than that of the naturally cooled samples.
- (2) Heating treatment can cause thermal damage to the granite sample and thus reduce the tensile strength and splitting modulus of the granite. With the increase of heating temperature, the tensile strength and splitting modulus decreased obviously. At the same heating temperature, the tensile strength and splitting modulus of the liquid-nitrogen-cooled sample were lower than those of the naturally cooled sample.
- (3) When the heating temperature was lower than 150 °C, the naturally cooled sample showed no obvious AE signals at low load levels. However, the ring-down counts of the liquid-nitrogen-cooled samples at a low load level were similar to that of the naturally cooled samples at a high load level. With the increase in heating temperature, the ring-down counts of the liquid-nitrogen-cooled samples were significantly higher than that of the naturally cooled samples.
- (4) When the heating temperature was less than 450 °C, the elastic energy stored in the liquid-nitrogen-cooled samples was lower than that stored in the naturally cooled samples under the same load level. When the heating temperature reached 600 °C, the elastic energy of the naturally cooled and liquid-nitrogen-cooled samples was close.
- (5) With the increase in heating temperature, the dissipated energy of high-temperature granite after both natural cooling and liquid-nitrogen cooling increases first and then decreases. Under the same heating temperature, the dissipated energy of high-temperature granite after natural cooling treatment was greater than that after liquid-nitrogen cooling treatment. At the same load level and heating temperature, the absorbed energy of the naturally cooled sample is greater than that of the liquid-nitrogen-cooled sample.
- (6) Overall, liquid-nitrogen cooling can bring significant thermal damage to high-temperature granite. After liquid-nitrogen cooling, microcracks in high-temperature granite increased and mechanical strength degraded. Consequently, microcracks easily expanded and propagated under external force.

Author Contributions: Methodology, C.C. and B.W.; conceptualization, C.C. and Z.Z.; investigation, C.C. and Z.T.; data curation, Y.F.; writing—original draft, C.C.; writing—review and editing, B.W. and C.C.; Funding acquisition, C.C. All authors have read and agreed to the published version of the manuscript.

Funding: This research was funded by the Fundamental Research Funds for the Central Universities of China University of Mining and Technology (Grant No. 2023KYJD1006).

Data Availability Statement: Data will be made available on request.

Conflicts of Interest: The authors declare no conflict of interest.

References

1. Zhou, Z.; Liu, S.; Liu, J. Study on the Characteristics and Development Strategies of Geothermal Resources in China. *J. Nat. Resour.* **2015**, *30*, 1210–1221.
2. Lei, H. Coupling Mechanics with Thermal-Hydrodynamic Processes for Heat Development in Enhanced Geothermal Systems (EGS). Ph.D. Thesis, Jilin University, Changchun, China, 2014.
3. Penny, G.S.; Conway, M.W.; Schraufnagel, R.A. The Evaluation of Proppant Transport and Cleanup of Foamed Fluids Used in Hydraulic Fracturing of Shallow, Water-Sensitive Reservoirs. In Proceedings of the SPE Eastern Regional Meeting, Pittsburgh, PA, USA, 2–4 November 1993; Society of Petroleum Engineers: The Woodlands, TX, USA, 1993.

4. Rozell, D.J.; Reaven, S.J. Water pollution risk associated with natural gas extraction from the Marcellus Shale. *Risk Anal.* **2012**, *32*, 1382–1393. [[CrossRef](#)]
5. Gregory, K.B.; Vidic, R.D.; Dzombak, D.A. Water management challenges associated with the production of shale gas by hydraulic fracturing. *Elements* **2011**, *7*, 181–186. [[CrossRef](#)]
6. Kim, K.M.; Kemeny, J. Effect of thermal shock and rapid unloading on mechanical rock properties. In Proceedings of the 43rd US Rock Mechanics Symposium & 4th US-Canada Rock Mechanics Symposium, Asheville North, CA, USA, 28 June–1 July 2009; American Rock Mechanics Association: Alexandria, VA, USA, 2009.
7. Shouldice, S.P. Liquid nitrogen developments and applications in drilling and completion operations. *J. Can. Pet. Technol.* **1964**, *3*, 158–164. [[CrossRef](#)]
8. Mcdaniel, B.W.; Grundmann, S.R.; Kendrick, W.D.; Wilson, D.R.; Jordan, S.W. Field applications of cryogenic nitrogen as a hydraulic fracturing fluid. In Proceedings of the SPE Annual Technical Conference and Exhibition, San Antonio, TX, USA, 8–10 October 1997; Society of Petroleum Engineers: The Woodlands, TX, USA, 1997.
9. Grundmann, S.R.; Rodvelt, G.D.; Dials, G.A. Cryogenic nitrogen as a hydraulic fracturing fluid in the Devonian Shale. In Proceedings of the SPE Eastern Regional Meeting, Pittsburgh, PA, USA, 9–11 November 1998; Society of Petroleum Engineers: The Woodlands, TX, USA, 1998.
10. Ren, S.; Fan, Z.; Zhang, L. Mechanisms and Experimental Study of Thermal-shock Effect on Coal-rock Using Liquid Nitrogen. *Chin. J. Rock Mech. Eng.* **2013**, *32*, 3790–3794.
11. Cai, C.; Li, G.; Huang, Z. Experiment of coal damage due to super-cooling with liquid nitrogen. *J. Nat. Gas Sci. Eng.* **2015**, *22*, 42–48. [[CrossRef](#)]
12. Cai, C.; Li, G.; Huang, Z. Experimental study of the effect of liquid nitrogen cooling on rock pore structure. *J. Nat. Gas Sci. Eng.* **2014**, *21*, 507–517. [[CrossRef](#)]
13. Cai, C.; Gao, F.; Li, G. Evaluation of coal damage and cracking characteristics due to liquid nitrogen cooling on the basis of the energy evolution laws. *J. Nat. Gas Sci. Eng.* **2016**, *29*, 30–36. [[CrossRef](#)]
14. Cai, C.; Gao, F.; Yang, Y. The effect of liquid nitrogen cooling on coal cracking and mechanical properties. *Energy Explor. Exploit.* **2018**, *36*, 1609–1628. [[CrossRef](#)]
15. Cha, M.; Yin, X.; Kneafsey, T. Cryogenic fracturing for reservoir stimulation-Laboratory studies. *J. Pet. Sci. Eng.* **2014**, *124*, 436–450. [[CrossRef](#)]
16. Cha, M.; Alqahtani, N.B.; Yao, B. Cryogenic fracturing of wellbores under true triaxial-confining stresses: Experimental investigation. *SPE J.* **2018**, *23*, 271–289. [[CrossRef](#)]
17. Cha, M.; Alqahtani, N.B.; Yin, X. Laboratory system for studying cryogenic thermal rock fracturing for well stimulation. *J. Pet. Sci. Eng.* **2017**, *156*, 780–789. [[CrossRef](#)]
18. Zhai, C.; Qin, L.; Liu, S. Pore Structure in Coal: Pore Evolution after Cryogenic Freezing with Cyclic Liquid Nitrogen Injection and Its Implication on Coalbed Methane Extraction. *Energy Fuels* **2016**, *30*, 6009–6020. [[CrossRef](#)]
19. Zhai, C.; Wu, S.; Liu, S. Experimental study on coal pore structure deterioration under freeze-thaw cycles. *Environ. Earth Sci.* **2017**, *76*, 1–12. [[CrossRef](#)]
20. Yao, B.; Wang, L.; Yin, X. Numerical modeling of cryogenic fracturing process on laboratory-scale Niobrara shale samples. *J. Nat. Gas Sci. Eng.* **2017**, *48*, 169–177. [[CrossRef](#)]
21. Zhang, S.; Huang, Z.; Li, G. Numerical analysis of transient conjugate heat transfer and thermal stress distribution in geothermal drilling with high-pressure liquid nitrogen jet. *Appl. Therm. Eng.* **2018**, *129*, 1348–1357. [[CrossRef](#)]
22. Zhang, S.; Huang, Z.; Wang, H. Thermal characteristics analysis with local thermal non-equilibrium model during liquid nitrogen jet fracturing for HDR reservoirs. *Appl. Therm. Eng.* **2018**, *143*, 482–492. [[CrossRef](#)]
23. Yang, R.; Huang, Z.; Shi, Y. Laboratory investigation on cryogenic fracturing of hot dry rock under triaxial-confining stresses. *Geothermics* **2019**, *79*, 46–60. [[CrossRef](#)]
24. Wu, X.; Huang, Z.; Song, H. Variations of Physical and Mechanical Properties of Heated Granite After Rapid Cooling with Liquid Nitrogen. *Rock Mech. Rock Eng.* **2019**, *52*, 2123–2139. [[CrossRef](#)]
25. Wu, X.; Huang, Z.; Zhang, S. Damage Analysis of High-Temperature Rocks Subjected to LN₂ Thermal Shock. *Rock Mech. Rock Eng.* **2019**, *52*, 2585–2603. [[CrossRef](#)]
26. Wu, X.; Huang, Z.; Cheng, Z. Effects of cyclic heating and LN₂-cooling on the physical and mechanical properties of granite. *Appl. Therm. Eng.* **2019**, *156*, 99–110. [[CrossRef](#)]
27. Hong, C.; Yang, R.; Huang, Z.; Zhuang, X.; Wen, H.; Hu, X. Enhance liquid nitrogen fracturing performance on hot dry rock by cyclic injection. *Pet. Sci.* **2023**, *20*, 951–972. [[CrossRef](#)]
28. Hou, P.; Gao, F.; Yang, Y. Effect of bedding plane direction on acoustic emission characteristics of shale in Brazilian tests. *Rock Soil Mech.* **2016**, *37*, 1603–1612.
29. Michlmayr, G.; Cohen, D.; Or, D. Sources and characteristics of acoustic emissions from mechanically stressed geologic granular media—A review. *Earth-Sci. Rev.* **2012**, *112*, 97–114. [[CrossRef](#)]
30. Liu, X. Study on the Deformation and Failure Characteristics and the Permeation Behavior of Gas-Saturated Coal. Ph.D. Thesis, China University of Mining and Technology, Xuzhou, China, 2013.
31. Zhang, Z. Energy Evolution Mechanism during Rock Deformation and Failure. Ph.D. Thesis, China University of Mining and Technology, Xuzhou, China, 2013.

32. Xie, H.; Ju, Y.; Li, L. Criteria for Strength and Structural Failure of Rocks Based on Energy Dissipation and Energy Release Principles. *Chin. J. Rock Mech. Eng.* **2005**, *24*, 3003–3010.
33. Cai, C.; Ren, K.; Tao, Z.; Xing, Y.; Gao, F.; Zou, Z.; Feng, Y. Experimental Investigation of the Damage Characteristics of High-Temperature Granite Subjected to Liquid Nitrogen Treatment. *Nat. Resour. Res.* **2022**, *31*, 2603–2627. [[CrossRef](#)]
34. Wang, X.Q.; Schubnel, A.; Fortin, J. Physical properties and brittle strength of thermally cracked granite under confinement. *J. Geophys. Res. Solid Earth* **2013**, *118*, 6099–6112. [[CrossRef](#)]
35. Horii, H.; Nemat-Nasser, S. Brittle Failure in Compression: Splitting, Faulting and Brittle-Ductile Transition. Philosophical Transactions for the Royal Society of London. *Ser. A Math. Phys. Sci.* **1986**, *139*, 337–374.
36. Lu, M.; Su, Y.; Zhan, S.; Almarbat, A. Modeling for reorientation and potential of enhanced oil recovery in refracturing. *Adv. Geo-Energy Res.* **2020**, *4*, 20–28. [[CrossRef](#)]

Disclaimer/Publisher's Note: The statements, opinions and data contained in all publications are solely those of the individual author(s) and contributor(s) and not of MDPI and/or the editor(s). MDPI and/or the editor(s) disclaim responsibility for any injury to people or property resulting from any ideas, methods, instructions or products referred to in the content.